

---

# STAGEWISE REINFORCEMENT LEARNING AND THE GEOMETRY OF THE REGRET LANDSCAPE

---

**Chris Elliott**<sup>=</sup>  
Timaeus

**Einar Urdshals**<sup>=</sup>  
Timaeus

**David Quarel**<sup>=</sup>  
Timaeus

**Matthew Farrugia-Roberts**  
University of Oxford

**Daniel Murfet**  
Timaeus

January 13, 2026

## ABSTRACT

Singular learning theory characterizes Bayesian learning as an evolving tradeoff between accuracy and complexity, with transitions between qualitatively different solutions as sample size increases. We extend this theory to deep reinforcement learning, proving that the concentration of the generalized posterior over policies is governed by the local learning coefficient (LLC), an invariant of the geometry of the regret function. This theory predicts that Bayesian phase transitions in reinforcement learning should proceed from simple policies with high regret to complex policies with low regret. We verify this prediction empirically in a gridworld environment exhibiting stagewise policy development: phase transitions over SGD training manifest as “opposing staircases” where regret decreases sharply while the LLC increases. Notably, the LLC detects phase transitions even when estimated on a subset of states where the policies appear identical in terms of regret, suggesting it captures changes in the underlying algorithm rather than just performance.

## 1 Introduction

What determines the kinds of agents that deep reinforcement learning will produce? This question is both scientifically fundamental and consequential for real-world deployment: the inductive biases of RL training may underlie phenomena relevant to AI alignment ranging from goal misgeneralization to reward hacking (Anwar et al., 2024, §2.5). Yet stochastic gradient descent, the workhorse of deep RL, remains difficult to analyze directly. In this paper we study a more theoretically tractable learning process, Bayesian inference of parametrized policies, and prove a result with surprising implications: *a more optimal policy is not always more optimal from a Bayesian perspective*. Bayesian learning involves an evolving tradeoff between the regret of a policy and the complexity of its parametrization, as measured by an invariant of the geometry of the regret function known as the local learning coefficient (Watanabe, 2009; Lau et al., 2025). For finite data, a simpler policy with higher regret can outcompete a complex policy with lower regret. Understanding this tradeoff may illuminate how simplicity biases shape the agents that emerge from training.

Our approach is indirect: rather than analyzing SGD trajectories, we characterize which policies are favored by Bayesian inference and then ask how this relates to the outcomes of stochastic optimization. This strategy splits a hard problem into two parts. The first part – understanding Bayesian learning for deep RL – is the focus of this paper. The second part – understanding the relationship between concentration of the posterior and SGD dynamics – remains open and is an important area for future work.

---

<sup>=</sup>These authors contributed equally to this work.

To develop a Bayesian theory of deep RL we must confront two difficulties. First, the data in RL is not identically distributed: trajectories depend on the agent’s actions, so different agents observe different trajectories. Second, neural network policies are *singular* statistical models, meaning the Fisher information matrix is not invertible and standard asymptotic results (such as the Bernstein-von Mises theorem) do not apply. Singular learning theory (SLT; Watanabe, 2009) provides the mathematical tools to handle this second difficulty. Our contribution is to extend these tools to the RL setting, where both difficulties are present.

In supervised learning, SLT predicts that Bayesian learning should exhibit *phase transitions*: as sample size increases, the posterior can shift abruptly from concentrating in one region of parameter space to another (Watanabe, 2009; Chen et al., 2024b, §7.6). These transitions reflect the evolving tradeoff between accuracy and complexity encoded in Watanabe’s free energy formula. As we will show, the free energy formula also applies in RL, which leads to three predictions. First, the posterior over policies should exhibit phase transitions: sudden shifts from simpler, higher-regret policies to more complex, lower-regret policies as the agent incorporates more trajectory data. Second, these Bayesian transitions should have observable consequences for SGD training, manifesting as plateaus in return punctuated by rapid transitions. Third, such transitions should be accompanied by increases in the local learning coefficient, our complexity measure. The empirical results of this paper validate all three predictions.

We make the following contributions:

- **We define a generalized posterior** over parameters for RL policies using importance sampling, connecting to the control-as-inference literature (Levine, 2018) and work of Bissiri et al. (2016) on belief updating (Section 2.4).
- **We prove that Watanabe’s free energy formula and WBIC theorem generalize** to this setting under some assumptions on the environment (Section 2), establishing that the local learning coefficient (LLC) governs posterior concentration. This gives a precise sense in which the geometry of the regret function  $G$  governs Bayesian learning for deep RL agents and allows us to make the aforementioned observation about more optimal policies (lower regret) not always being more optimal from a Bayesian perspective (higher posterior concentration), see Section 2.7.
- **We use these results to derive a theoretical prediction:** Bayesian phase transitions in RL should proceed from simple, high-regret policies to complex, low-regret policies (Section 2.7).
- **We verify this prediction empirically** in a gridworld environment exhibiting stagewise learning, with “opposing staircases” of decreasing regret and increasing complexity (Figure 1).
- **We show that the LLC estimator detects phase transitions** even when evaluated on a subset of states where the policies have identical regret, suggesting it captures algorithmic rather than purely behavioral changes (Section 3.4.4).

The remainder of the paper is organized as follows. Section 2 develops the theoretical foundations, defining the generalized posterior and proving our main theorem. Section 3 gives the empirical results: Section 3.2 presents the environment and the agent trained to solve it, Section 3.3 explains how we estimate the LLC and Section 3.4 presents our study of phase transitions. In Section 4 we review related work, and in Section 5 we return to discuss how these theoretical results allow us to think at a high-level about the kinds of agents that deep reinforcement learning will produce.

## 2 Theory

### 2.1 Background

By the Bayesian learning process we mean how the posterior distribution  $p(w|D_n)$  over parameters  $w \in W$  given data  $D_n$  (e.g. observed trajectories in an RL setting) evolves as  $n$  increases. In supervised learning for “regular” models, where the data consists of  $n$  random variables sampled independently and identically and the Fisher information matrix is invertible, the story is simple: the posterior converges as  $n \rightarrow \infty$  to a normal distribution centered on the maximum likelihood estimator with variance controlled by the (inverse of the) Fisher information matrix (by the Bernstein-von Mises theorem, see Hartigan, 1983).

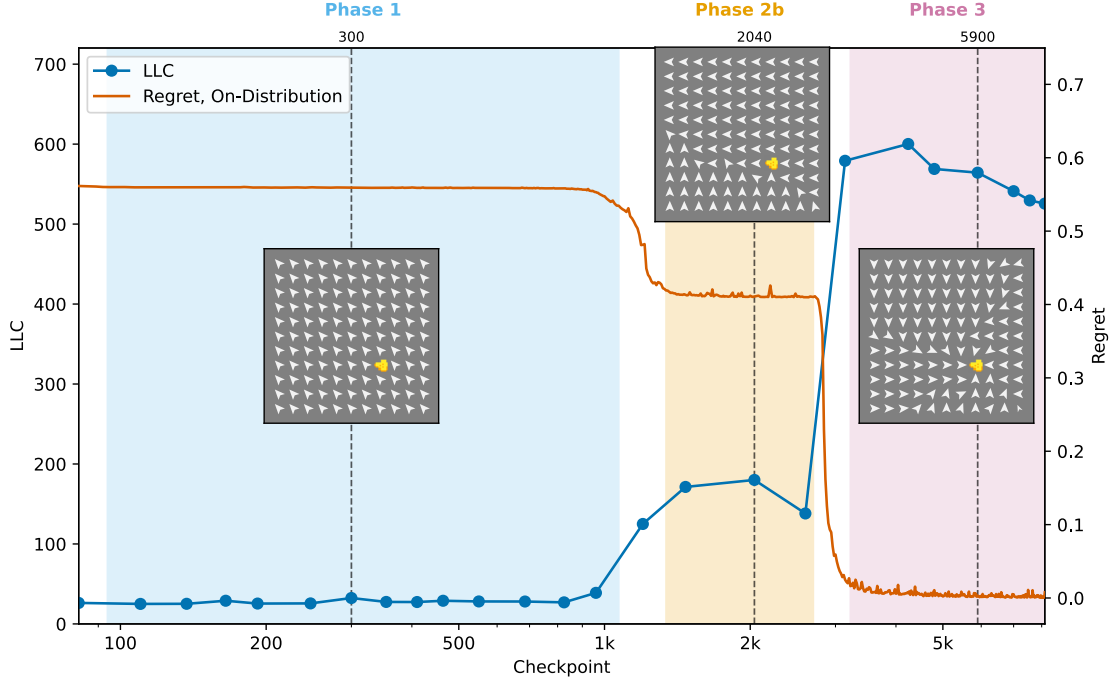


Figure 1: **Opposing staircases of regret and complexity:** Comparison of the regret and complexity (as estimated by the local learning coefficient) across training for an agent optimized to follow shortest paths towards the goal location (cheese), which was located in the top-left corner in  $\sim \frac{1}{3}$  of sampled episodes and uniformly across all locations in the remaining episodes. Phases are indicated along with visualizations of policies at the indicated checkpoints (i.e. policy gradient steps). In the first phase the agent moves up and left with equal probability; in the second phase it moves deterministically towards the top-left region, passing through the goal if possible, and finally in the third phase it moves directly toward the goal. For each location  $s$ , the arrow drawn points in the direction of the vector  $v_s = [\pi(\rightarrow|s, \emptyset) - \pi(\leftarrow|s, \emptyset), \pi(\uparrow|s, \emptyset) - \pi(\downarrow|s, \emptyset)]$  and has size proportional to  $\|v_s\|_1$  representing the expected direction of movement if the agent spawns in cell  $s$ . Policy representation taken from Mini et al. (2023). Phase transitions are associated with rapid decreases in regret and rapid increases in the LLC estimate.

However, the study of Bayesian learning for deep RL differs in two important ways from this simple story:

- **Non-identically distributed data:** in RL the data from which an agent learns optimal behavior is typically a set of *trajectories*  $o_0, a_0, r_0, o_1, a_1, r_1 \dots$  consisting of actions  $a$ , observations  $o$  and rewards  $r$ . This source is *not* identically distributed, as the actions of the agent shape the distribution of trajectories: for example in a video game, more experienced agents may gain access to new parts of the environment
- **The model is singular rather than regular:** when we parametrize our statistical model (in the case of RL, our policy) by a neural network the Fisher information matrix is not invertible and the model is *not* regular. This is the typical situation in deep learning Watanabe (2007); Wei et al. (2022b). Statistical models which are not regular are called *singular* and the appropriate mathematical framework for studying the Bayesian learning process for supervised learning is singular learning theory (SLT; Watanabe (2009)) which introduces ideas from algebraic geometry.

These two factors imply that a mathematical theory of parametric Bayesian learning which is general enough to treat deep RL must be nontrivial. Indeed, such a theory does not currently exist. The first contribution of this paper is to establish such a theory, in this section. The burden of additional mathematical sophistication has an upside: **the Bayesian learning process is more interesting.**

In supervised learning it is known that the posterior for singular models, rather than converging to a normal distribution as in the regular case, can “jump” at certain critical sample sizes  $n^*$  from concentrating in

one region of parameter space for  $n < n^*$  to concentrating in another region for  $n > n^*$ . This behavior resembles phase transitions in statistical physics (Watanabe, 2009, §7.6). In short, **SLT for supervised learning predicts that the Bayesian learning process should involve phase transitions**. This has been verified for Bayesian learning in small models (Chen et al., 2024b) and is conjecturally related to stagewise learning in SGD training in a range of systems including transformers (Hoogland et al., 2025). These phase transitions are explained by a theorem Watanabe (2013) that characterizes the optimal tradeoff between how well a model fits the data (accuracy) and its complexity, measured by a key quantity in SLT known as the local learning coefficient (LLC; Lau et al. (2025)). Stagewise learning has also been observed in deep reinforcement learning (Clift et al., 2020; McGrath et al., 2022).

## 2.2 Details

We will begin by discussing the foundational results on which our complexity measure for deep reinforcement learning models is based: a generalization of the theory of singular learning as developed by Watanabe (2009; 2018) from distribution learning to a more general class of problems.

We will state our results for finite Markov decision problems in this setting, however the assumption of finiteness is not necessary; we treat a more general case in Appendix E. Our results also apply beyond the Markov decision problem setting to a general generalized Bayesian learning context that encompasses both reinforcement and supervised learning.

## 2.3 Setup

We will study a partially observable finite Markov decision process with sets  $\mathcal{S}, \mathcal{A}$  and  $\mathcal{O}$  of states, actions and observations respectively. Denote the transition function of the Markov problem by <sup>1</sup>

$$p: \mathcal{S} \times \mathcal{A} \rightarrow \Delta(\mathcal{S} \times \mathcal{O} \times \mathbb{R})$$

and suppose that the expected value of the return associated to each state-action pair is finite. Fix a maximum episode length  $T_{\max}$ . A *trajectory* is a finite sequence

$$\tau = (s_0, o_0, a_1, s_1, o_1, \dots, a_{T_{\max}}, s_{T_{\max}}, o_{T_{\max}})$$

where  $s_i \in \mathcal{S}, o_i \in \mathcal{O}$  and  $a_i \in \mathcal{A}$ . We write  $\mathcal{T}$  for the finite set consisting of all trajectories.

Let  $\gamma \in [0, 1]$  denote the discount factor. Let  $r(s, a)$  denote the expected reward in state  $s \in \mathcal{S}$  for action  $a \in \mathcal{A}$ . The *return* of a trajectory  $\tau \in \mathcal{T}$  is given by

$$r(\tau) = \sum_{i=1}^{T_{\max}} \gamma^i r(s_{i-1}, a_i),$$

where we note the reuse of the symbol  $r$ , this will not lead to ambiguity since we will not need to refer to the expected return of a state-action pair again.

Consider a real analytic family  $\{\pi_w\}$  of policies for the Markov problem parameterized by  $w \in W$ . This family, together with the transition function  $p$  and a distribution  $\Lambda$  over initial states, determines a family  $\{q_w\}$  of probability distributions on the set  $\mathcal{T}$  of trajectories defined by

$$q_w(\tau) = \Lambda(s_0)p(o_0|s_0) \prod_{i=1}^{T_{\max}} \pi_w(a_i|o_{i-1})p(s_i|a_i)p(o_i|s_i).$$

We can now define our optimization objective: the *expected return* at parameter  $w \in W$  is  $R(w) = \mathbb{E}_{\tau \sim q_w}(r(\tau))$ . Let  $R_{\max} = \sup_{w \in W} R(w)$ . The *regret* at parameter  $w \in W$  is

$$G(w) = R_{\max} - R(w).$$

It will be convenient to write the regret in the alternative form  $\mathbb{E}_{\tau \sim q_w}(g(\tau))$  where  $g(\tau) = R_{\max} - r(\tau)$ .

<sup>1</sup>One usually imposes restrictions on the transition function  $p$ , in particular the condition that the observation depends only on the output state.

## 2.4 The Generalized Posterior

In reinforcement learning the goal of a learner is to acquire information about the environment in order to act optimally, which means maximizing the reward  $R(w)$ . In Bayesian statistics the goal of a learner is to predict and it is *a priori* unclear how to incorporate scalar rewards into this framework. In addition to this problem we also need to specify what kind of observations about the environment we are learning from.

In this paper we adopt the following two positions:

1. **Reward vs probability:** we follow the *Kalman–Todorov* duality Kalman (1960); Todorov (2008), which relates optimal control to optimal prediction under the following conceptual relation

$$\text{Probability} \propto e^{-\text{Cost}}. \quad (1)$$

This has been studied more recently under the name “control as inference” (Levine, 2018).

2. **Nature of observations:** an agent learns from observing the consequences of its actions, and thus it is obvious that *trajectories* should be the “samples” in a Bayesian approach to RL. However, unlike supervised learning, these observations are tied to the learner whose policy generates the actions. Moreover, it seems reasonable to acquire information about the environment from the experience of similar agents (including the agent itself, earlier in the learning process). Accordingly, we take

$$D_n = \{(w_i, \tau_i)\}_{i=1}^n, \quad \tau_i \sim q_{w_i} \quad (2)$$

as our model of the dataset where  $w_1, \dots, w_n$  is any sequence of points in  $W$  and  $\tau_1, \dots, \tau_n$  is a sequence of random variables in  $\mathcal{T}$  where  $\tau_i$  is sampled from the distribution  $q_{w_i}$ . This formulation encompasses both off-policy data (distinct  $w_i$ ) and on-policy data (all  $w_i = w_0$  for a fixed  $w_0$ ). Note that these random variables are independent but not identical, since we allow  $w_i \neq w_j$ .

Given a prior  $\phi(w)$  over parameters for policies, to complete a Bayesian description of reinforcement learning it only remains to define how this distribution is updated given observations  $D_n$ . That is, we need to define a *generalized posterior*  $p(w|D_n)$ . Since  $g(\tau)$  is our cost function and the  $\tau_i$  are independent, (1) gives in the on-policy case (where  $w_i = w_0$  for  $1 \leq i \leq n$ )

$$p(D_n|w_0) = \prod_{i=1}^n p(\tau_i|w_0) = \prod_{i=1}^n e^{-g(\tau_i)} = e^{-nG_n(w_0)}$$

where  $G_n(w_0) = \frac{1}{n} \sum_{i=1}^n g(\tau_i)$ . However we can’t use Bayes rule to obtain  $p(w|D_n)$ , because we can only define  $p(D_n|w)$  this way for  $w = w_0$ . To proceed note that  $G_n(w_0)$  is a Monte Carlo estimator for

$$G(w_0) = \mathbb{E}_{\tau \sim q_{w_0}} [g(\tau)].$$

The *Kalman–Todorov* principle (1) suggests that we should assign likelihood

$$p(D_n|w) \propto \exp(-n \hat{G}_n(w)), \quad (3)$$

where  $\hat{G}_n(w)$  is an empirical estimate of the population regret

$$G(w) = \mathbb{E}_{\tau \sim q_w} [g(\tau)] = \sum_{\tau \in \mathcal{T}} q_w(\tau) g(\tau).$$

The issue is that, when  $\tau_i \sim q_{w_i}$ , the naive average  $\frac{1}{n} \sum_i g(\tau_i)$  estimates  $\frac{1}{n} \sum_i \mathbb{E}_{\tau \sim q_{w_i}} [g(\tau)]$ , which depends on the behavior policies and is not, in general, equal to  $G(w)$  for a counterfactual candidate  $w$ . To address this, fix  $i$  and suppose  $q_w$  is absolutely continuous with respect to  $q_{w_i}$  (that is,  $q_{w_i}(\tau) = 0$  implies  $q_w(\tau) = 0$  for all  $\tau \in \mathcal{T}$ ), so that the Radon–Nikodym derivative  $\frac{dq_w}{dq_{w_i}}(\tau)$  is well-defined. Since  $\mathcal{T}$  is finite in our setting, this derivative is simply the likelihood ratio  $\frac{q_w(\tau)}{q_{w_i}(\tau)}$ . Then for any function  $f: \mathcal{T} \rightarrow \mathbb{R}$ ,

$$\mathbb{E}_{\tau \sim q_w} [f(\tau)] = \mathbb{E}_{\tau \sim q_{w_i}} \left[ \frac{q_w(\tau)}{q_{w_i}(\tau)} f(\tau) \right].$$

Applying this with  $f = g$  yields

$$G(w) = \mathbb{E}_{\tau \sim q_w} [g(\tau)] = \mathbb{E}_{\tau \sim q_{w_i}} \left[ \frac{q_w(\tau)}{q_{w_i}(\tau)} g(\tau) \right]. \quad (4)$$

In other words, if  $\tau_i \sim q_{w_i}$  then the random variable

$$\frac{q_w(\tau_i)}{q_{w_i}(\tau_i)} g(\tau_i)$$

is an unbiased estimator of  $G(w)$ . Averaging across independent (but not identically distributed) samples therefore yields the canonical importance-sampling estimator

$$G_n(w) = \frac{1}{n} \sum_{i=1}^n \frac{q_w(\tau_i)}{q_{w_i}(\tau_i)} g(\tau_i), \quad \text{for which } \mathbb{E}[G_n(w) \mid w_1, \dots, w_n] = G(w). \quad (5)$$

Observe that  $G_n(w)$  can be computed without knowledge of the environment's transition function: writing

$$q_w(\tau) = q_{\text{env}}(\tau) \prod_{t=1}^{T_{\max}} \pi_w(a_t \mid o_{t-1}),$$

where  $q_{\text{env}}(\tau)$  denotes the product of all policy-independent environment terms, we obtain

$$\frac{q_w(\tau)}{q_{w_i}(\tau)} = \prod_{t=1}^{T_{\max}} \frac{\pi_w(a_t \mid o_{t-1})}{\pi_{w_i}(a_t \mid o_{t-1})}.$$

Thus the importance weight can be computed from action probabilities under the candidate and behavior policies; all environment-dependent factors cancel. Combining (3) with (5) leads to the definition

$$p(w \mid D_n) = \frac{1}{Z} \exp(-nG_n(w)) \phi(w) \quad (6)$$

where the normalizing constant  $Z$  is chosen so that this is a probability distribution. Note that this reduces to the on-policy calculation above when  $w_i = w_0$  for all  $i$  and  $\beta = 1$ . We will also need to introduce a tempered version of this posterior, and notation for the probability of an open set according to the posterior:

**Definition 2.1.** Fix a constant  $\beta > 0$  and an analytic prior distribution  $\phi$  on  $W$ . The *generalized tempered posterior distribution* (or Gibbs posterior) is the probability distribution on  $W$  defined by

$$\mu_n^\beta(U) = \frac{Z_{n,\beta}(U)}{Z_{n,\beta}(W)}$$

where  $Z_{n,\beta}(U) = \int_U \exp(-n\beta G_n(w)) \phi(w) dw$

for open sets  $U \subseteq W$ . We call  $Z_{n,\beta}(U)$  the *evidence* of the subset  $U$  and  $F_{n,\beta}(U) = -\log Z_{n,\beta}(U)$  the *free energy*. Both of these quantities measure the concentration of the generalized posterior in  $U$ .

For more discussion of the generalized posterior see Section E.2.

## 2.5 Main Theoretical Results

With the above definition of the generalized posterior  $p(w \mid D_n)$  the study of the Bayesian learning process in RL reduces to the following mathematical question: where does the generalized posterior concentrate? This is captured by  $\mu_n^\beta(U)$  which depends on the random variable  $D_n$ , and we give precise answers in terms of the asymptotic behaviour of the free energy  $F_{n,\beta}(U)$ . More precisely, we prove that the large  $n$  behavior of the generalized posterior is controlled by the singular geometry of the set  $W_0 \subseteq W$  of optima.

Our results generalize Watanabe (2018, Section 6.3) and Watanabe (2013, Theorem 4) to RL.

**Assumption 2.2.** Our main theorem will require imposing the following condition on a Markov decision problem. If  $w \in W$  is an optimal parameter, we will assume that  $g(\tau) = 0$  almost-always for the distribution  $q_w$ . In other words *optimal policies almost always receive optimal return*. This is true, for example, if the transition function is deterministic.

**Theorem 2.3.** Consider a Markov decision problem satisfying Assumption 2.2. Then the generalized posterior obeys the following conditions:

1. *Asymptotics of the posterior:* Let  $U \subseteq W$  be an open set. The generalized tempered posterior has asymptotic behavior

$$Z_{n,\beta}(U) = \int_U \exp(-n\beta G_n(w))\phi(w)dw \sim n^{-\lambda(U)} \log n^{m(U)-1}$$

where  $\lambda(U), m(U)$  are the learning coefficient and multiplicity of  $G$  on the set  $U$ <sup>2</sup>.

2. *Expectation of the total loss:* Let  $w_0$  be a local minimum of  $G$ . Let  $\mathbb{E}_n^\beta$  represent the expected value with respect to the tempered posterior  $\mu_n^\beta$ . Let  $\beta$  be a positive function on the natural numbers such that  $\beta(n)$  converges as  $n \rightarrow \infty$ . Then there exists an open neighborhood  $U'$  of  $w_0$  so that for all subneighborhoods  $U \subseteq U'$

$$\mathbb{E}_n^\beta(nG_n(w)|_U) = nG_n(w_0) + \frac{\lambda(U)}{\beta} + o_P(\log n).$$

*Proof.* See Appendix E, specifically E.2.4 and E.2.5.  $\square$

## 2.6 The Local Learning Coefficient

Given a point  $w^*$  in parameter space with open neighborhood  $U$ , according to Theorem 2.3 we may identify  $\lambda(U)$  as

$$\lambda(U) = n\beta \left[ \mathbb{E}_{n,U}^\beta[G_n(w)] - G_n(w^*) \right], \quad (7)$$

where  $\mathbb{E}_{n,U}^\beta$  is the expectation with respect to the tempered posterior restricted to the open set  $U$ . We may, if we like, obtain the *local* learning coefficient at the point  $w^*$  by shrinking the neighborhood  $U$ , for instance if  $W$  is a subspace of  $\mathbb{R}^d$  then we can take a limit over balls of diminishing radius

$$\lambda(w^*) = \lim_{\varepsilon \rightarrow 0} \lambda(B_\varepsilon(w^*)).$$

More geometrically one can equivalently realize the local learning coefficient in terms of the asymptotic growth rate of basin volumes around a local minimum (see (Lau et al., 2025, §3.1)).

Theorem 2.3 explains how the local learning coefficient controls model selection during the learning process. Taking  $\beta = 1/\log n$  and writing  $F_n = F_{n,1}$ , Parts (1) and (2) of Theorem 2.3 together imply (see Definition E.44) the *free energy formula* for a local minimum  $w_0$  of  $G$

$$F_n(U) = nG_n(w_0) + \lambda(U) \log n + o_P(\log n) \quad (8)$$

where  $U$  is a sufficiently small open neighborhood of  $w_0$ . This formula describes the concentration of the posterior in a region  $U$  in terms of two invariants: the empirical regret  $G_n(w_0)$  (lower regret means lower  $F_n(U)$ , hence higher  $Z_n(U)$  and thus posterior concentration) and the learning coefficient  $\lambda$  (lower  $\lambda$  means a simpler parametrized policy, and higher posterior concentration). The prior  $\phi(w)$  contributes to the free energy, and thus posterior concentration, only through constant order terms. These can certainly play a significant role for low  $n$ , but we do not consider this explicitly there.

## 2.7 Implications of the free energy formula

The central insight for Bayesian learning in deep RL that we draw from the free energy formula (8) is that learning consists of an evolving tradeoff between *regret* and *complexity*. This is the translation to the setting of RL of a perspective due to Watanabe (2009, §7.6), see also (Balasubramanian, 1997; Chen et al., 2024b).

Let  $w_1, w_2$  be two local minima of the regret  $G$  with respective local neighborhoods  $U_1, U_2$ . To compare the concentration of the posterior in these two regions we compute the likelihood ratio (setting  $\beta = 1$ )

$$\frac{\mu_n(U_1)}{\mu_n(U_2)} = \frac{Z_n(U_1)}{Z_n(U_2)}$$

<sup>2</sup>The quantities  $\lambda(U)$  and  $m(U)$  are referred to respectively by algebraic geometers as the real log canonical threshold and the real log canonical multiplicity of the function  $G$  restricted to the set  $U$ .

which is greater or less than one according to the sign of negative logarithm (which is negative if  $U_1$  is more preferred than  $U_2$ ), which has asymptotic expansion

$$\begin{aligned} F_n(U_1) - F_n(U_2) &= (nG_n(w_1) + \lambda(U_1) \log n - (nG_n(w_2) + \lambda(U_2) \log n + o_P(\log n)) \\ &= n(G_n(w_1) - G_n(w_2)) + (\lambda(U_1) - \lambda(U_2)) \log n + o_P(\log n) \\ &= n\delta G - \delta\lambda \log n + o_P(\log n) = \left( \frac{n}{\log n} \delta G - \delta\lambda + o_P(1) \right) \log n. \end{aligned}$$

where  $\delta G = G_n(w_1) - G_n(w_2)$  and  $\delta\lambda = \lambda(U_2) - \lambda(U_1)$ . From this we infer the following:

- **Observation 1:** if  $\delta G > 0$  then for  $n$  large the posterior prefers  $U_2$  (the lower regret solution).
- **Observation 2:** if  $\delta G > 0$  and  $\delta\lambda > 0$  then the posterior may prefer  $U_1$  for small  $n$  (a higher regret, but simpler, parametrized policy can outcompete a lower regret policy).
- **Observation 3:** if  $\delta G > 0$  and  $\delta\lambda > 0$  then there exists a *critical dataset size*  $n^*$  such that the posterior prefers  $U_1$  for  $n < n^*$  and  $U_2$  for  $n > n^*$ . This  $n^*$  is the solution<sup>3</sup> of

$$\frac{n^*}{\log n^*} = \frac{\delta\lambda}{\delta G}.$$

Note that since the relationship between the free energy and the posterior is exponential, these switches in the sign of the free energy as a function of  $n$  can translate to rapid changes in posterior concentration. Following Watanabe (2018) and Chen et al. (2024b) we refer to these sudden shifts in the concentration of the posterior as *Bayesian phase transitions*.

This suggests a picture of the Bayesian learning process as a series of phase transitions, where the posterior jumps between neighborhoods of local minima  $w_i$  of  $G$ , according to a changing tradeoff between  $G$  and  $\lambda$  in the free energy formula. The most typical transition decreases  $G$  and increases  $\lambda$  (the posterior is willing, at some dataset size, to pay the free-energetic cost of higher complexity to get lower regret).

This is not that surprising if we think of learning as the process of incorporating information from observed trajectories into the network parameter, but framed differently it has a counter-intuitive implication, flagged already in the introduction: given any finite number of observed trajectories, a *more optimal policy* (lower regret) may not be *more optimal from a Bayesian perspective* (lower free energy) according to the concentration of the generalized posterior. This has implications for AI alignment, which we review in Section 5.3.

### 3 Empirical Results

Building upon the theoretical foundations, we wish to demonstrate that estimators for the local learning coefficient can be used to provide an effective complexity measure that tracks stagewise development of reinforcement learning models. We will demonstrate this in a toy model that nevertheless exhibits phase transitions during training and with respect to the variation of hyperparameters.

#### 3.1 Summary

We study a simple gridworld reinforcement learning problem in which an agent is incentivized to find a shortest path between two locations in a grid, and study the training dynamics of a deep neural network parameterizing this problem under policy gradient optimization. There are two key hyperparameters that we vary.

- $\gamma \in [0, 1]$ , the *discount rate*.

---

<sup>3</sup>We are ignoring the  $o_P(1)$  term in this presentation of phase transitions. Whether or not this is reasonable is hard to address theoretically, and we treat it as an empirical question. It is possible to eliminate a Bayesian phase transition, or delay it, by changing the prior in  $U_1, U_2$ .

- $\alpha \in [0, 1]$ , the mixing parameter for our initial state distribution. The initial state distribution is set to  $\alpha \Lambda_{\text{uniform}} + (1 - \alpha) \Lambda_{\text{corner}}$  where in  $\Lambda_{\text{uniform}}$  the goal is uniformly distributed over all possible squares in the grid and in  $\Lambda_{\text{corner}}$  it is always in the top-left corner.

During training we see stagewise development in policy space: the model transitions between plateaus in which the regret is roughly constant, the policy remains in a fixed region with qualitatively consistent behavior and the transitions between plateaus are relatively rapid. We refer to periods where the regret is approximately constant as *phases* and transitions between them as *phase transitions* (and one might compare this phenomenon to the phase transition seen in a toy model of supervised learning in Chen et al. (2024b)). For example, we will discuss some of the following common phases in policy space below.

- *Phase 1*: in all cases move up with probability 0.5 and left with probability 0.5.
- *Phase 2a*: move in a deterministic direction either up or left towards the goal, independent of the goal location.
- *Phase 2b*: move in a deterministic direction either up or left in a way that always moves towards to goal if possible.
- *Phase 3*: move deterministically towards the goal location.

We characterize a model as behaving according to one of these phases automatically – each phase describes a subspace of policy space and we characterize a phase as present when the  $L^2$  distance from this region is less than a cutoff value (0.15 times the maximum distance in the policy polytope.)

**Remark 3.1.** As  $\gamma$  becomes smaller transitioning away from phase 1 becomes increasingly incentivized, since a smaller  $\gamma$  leads to  $\gamma^n$  much more rapidly decaying to zero as a function of  $n$ . This means that paths that are much shorter dominate.

As  $\alpha$  becomes larger, transitioning away from phases 1 and 2a is increasingly incentivized since it is much more likely that the goal location will be distributed uniformly rather than only found in the top-left corner. So too for transitioning from phase 2b to phase 3.

In our experiments we estimate how the value of the LLC (which acts as our measure of complexity) changes during training and how it is affected by variation in hyperparameters  $\alpha$  and  $\gamma$ . We observe the following and refer to Section 3.4 for more details.

1. Phase transitions are accompanied by rapid increases in the LLC estimator, and later phases correspond to larger LLCs.
2. We see gradual decrease in the LLC estimate within phases 2 and 3 – the policy, and therefore the regret, does not change significantly but the representation of the policy within parameter space does change. The LLC of phase 1 exhibits a consistent value of  $41.5 \pm 8.2$  during training and across values of  $\alpha$  and  $\gamma$ .
3. The LLC detects phase transitions even when they are not visible from the loss alone. Indeed, we may estimate the LLC in states corresponding to the  $\alpha = 0$  distribution in which the goal is always in the top-left corner. Even if only these states are seen during estimation we still see rapid increases in the LLC estimator upon the phase transition.

## 3.2 Environment and Agent

### 3.2.1 Environment

We make use of a simplified version of the *Cheese in the Corner* (CITC) environment described in Abdel Sadek et al. (2025). The environment is a grid of size  $13 \times 13$  with a border of walls around the edge (leaving a  $11 \times 11$  grid of empty cells that can be navigated). One of the central  $11 \times 11$  cells contains the goal location (the *cheese*), and another contains the initial location for the agent (the *mouse*). All of the other cells are empty. The mouse can be moved in any one of the four cardinal directions, and if the move would cause the mouse to collide with a wall, the location of the mouse is unchanged. The objective is to move the mouse to the cell containing the cheese.

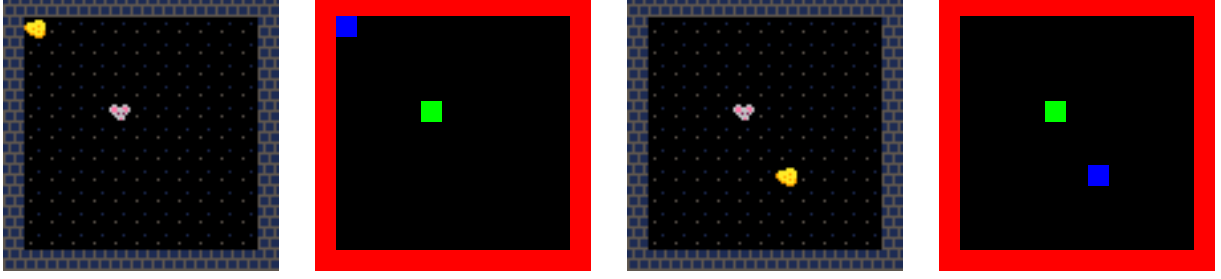


Figure 2: Two possible states the environment can be in, together with the observation seen by the agent.

The episode ends either when the mouse moves into the same cell as the cheese, and receives  $+1$  return for doing so, or when the environment times out after  $T_{\max}$  timesteps. On all other timesteps the return is  $0$ . The agent is incentivized to maximize the standard expected discounted return, given by  $\mathbb{E}_{\tau \sim q_w} [\sum_{t=1}^{\infty} \gamma^{t-1} r(s_t)] = \mathbb{E}_{\tau \sim q_w} [r(s_1) + \gamma r(s_2) + \dots]$  where  $\gamma$  is the discount factor and  $r(s_t)$  is the return associated to the state at timestep  $t$ . Therefore for a trajectory that reaches the cheese after  $T$  steps the return received by the agent is  $\gamma^{T-1}$  if  $T \leq T_{\max}$  and  $0$  otherwise.

The state seen by the agent is a tensor of shape  $(13 \times 13 \times 3)$ , where the third dimension is a one-hot encoding of the presence of a wall ( $[1, 0, 0]$ ), the mouse ( $[0, 1, 0]$ ), and the cheese ( $[0, 0, 1]$ ). An empty cell is encoded as  $[0, 0, 0]$ . There are  $(11 \times 11) \times (11 \times 11 - 1) = 14,520$  possible states the CITC environment can be in (though given that the cheese cannot move, the state space partitions into  $11^2$  possible connected subsets). We vary the distribution over the choice of cheese location to see the effects on the policies learned by the model during training.

We consider the initial state distributions:

- $\Lambda_{\text{corner}}$ : The goal always spawns in the top left corner and the starting location is distributed uniformly over all other cells.
- $\Lambda_{\text{uniform}}$ : The goal and the starting location are distributed uniformly over all distinct pairs of cells.
- $\Lambda_{\alpha}$ : The initial state is sampled from  $\Lambda_{\text{corner}}$  with probability  $1 - \alpha$  and from  $\Lambda_{\text{uniform}}$  with probability  $\alpha$ . We will write  $\Lambda_{\alpha} = (1 - \alpha)\Lambda_{\text{corner}} + \alpha\Lambda_{\text{uniform}}$  to indicate that  $\Lambda_{\alpha}$  is a mixture distribution.

We call  $\alpha$  the *mixing parameter* for the initial state distribution.

### 3.2.2 Model

The architecture of the model directly follows that used for Abdel Sadek et al. (2025), which itself is a modified version of the *Large* architecture described in Espeholt et al. (2018): A convolutional network with 15 convolutional layers, but the LSTM that normally follows is replaced by a simple feedforward network that takes both the output from the convolutional block, and a one-hot encoding of the previous action. Full details of the architecture are given in Espeholt et al. (2018).

Note that the inclusion of the previous action makes the model Markovian as a function of a state and previous action pair,  $a_t \sim \pi(\cdot | s_t, a_{t-1})$ .

The model itself is trained using standard vanilla REINFORCE with no baseline. A batch of levels is sampled from the environmental distribution  $\Lambda_{\alpha}$ , for which a trajectory for each is generated via interaction with the model. Actions are sampled on-distribution from the output of the model. The policy is then updated from the sampled trajectories using the gradient estimator

$$\frac{1}{B} \sum_{i=1}^B \sum_{t=1}^T r(\tau_{i, \geq t}) \log \pi_w(a_{i,t} | s_{i,t}, a_{i,t-1}) \quad (9)$$

where  $r(\tau_{i, \geq t}) = \sum_{j=t}^T \gamma^{j-t} r(s_{i,j}, a_{i,j-1})$  is the *reward-to-go* at time  $t$  associated to the  $i^{\text{th}}$  trajectory  $\tau_i = (s_{i,1}, a_{i,1}, \dots, s_{i,T})$ . We vary both the environmental distribution parameter  $\alpha$  as well as the discount rate  $\gamma$ .

to study the effects on the policies learned by the model during training. The batch size  $B$  and trajectory length  $T$  are given in Table 1.

Given the simplicity of the environment and given that there are only  $121 \times 120 \times 5 = 72600$  possible combinations<sup>4</sup> of state and previous action  $(s_t, a_{t-1})$  we can analytically compute the optimal reward  $R_{\max}$  and the exact reward  $R(w)$  of a given current policy  $\pi_w$ . This allows us to analytically compute the regret,  $G(w) = R_{\max} - R(w)$  during various stages of training, as well as visualize the policy for each possible location of the agent given a goal location.

### 3.3 Details of LLC Estimation

We define an *estimator* for the local learning coefficient (see Definition 2.6) using the preconditioned stochastic gradient Langevin dynamics (pSGLD) algorithm Li et al. (2015) to estimate sampling from the Gibbs posterior. This combines RMSNorm-style adaptive step sizes with SGLD Welling and Teh (2011). Rather than imposing the sharp cutoff associated to the restriction to a neighborhood we use a Gaussian prior centered at  $w^*$  with variance  $\sigma^2$ . The Gibbs posterior then takes the form

$$p(w|w^*, \beta, \sigma^2) \propto \exp \left\{ -n\beta G_{n,\alpha}(w) - \frac{1}{2\sigma^2} \|w - w^*\|_2^2 \right\}. \quad (10)$$

The hyperparameters are the sample size  $n$ , the inverse temperature  $\beta$ , which controls the contribution of the regret, and the variance  $\sigma^2$ , which controls proximity to  $w^*$ . For more details on these hyperparameters, see Watanabe (2013); Lau et al. (2025); Hoogland et al. (2025). In *loc. cit.* the inverse of the variance  $\sigma^2$  is referred to as the *localization strength*. Details of the hyperparameters used for LLC estimation can be found in Section B.

**Remark 3.2** (Off-distribution LLC estimation). The interpretation of the LLC estimator as an approximation to the true LLC makes sense near any local minimum  $w^* \in W$  of the loss function  $G$ . We observe that even though our loss (the regret function) depends on the hyperparameters  $\alpha$  and  $\gamma$ , as long as  $\alpha, \gamma \in (0, 1)$  the subspace of global minima, and the subspaces associated to the intermediate phases discussed below, will be independent of the hyperparameters. Therefore it makes sense to compute the LLC estimator of a trained model with respect to *different* values of  $\alpha, \gamma$  to those that were used during training. In particular we may make direct comparisons of the LLC estimates of models trained with different hyperparameter values by estimating LLC using a fixed loss function.

### 3.4 Phase Transitions

An *optimal policy*  $\pi^*$  for this environment is any policy where the agent moves closer to the goal with probability one. Any policy that performs a different strategy must be suboptimal for all mixing parameters  $\alpha$  such that  $0 < \alpha \leq 1$  and for all discount rates  $0 < \gamma < 1$ .<sup>5</sup> We note that optimal policies are not unique for this environment, as there are in general many possible paths from the agent to the goal.

We are interested in the dynamics of the training process itself and how the learned policy changes over time as a function of the mixing parameter  $\alpha$  and the discount rate  $\gamma$ . We observed that the training process itself exhibits *phase transitions* in policy space: the policy is stable for a long period of training before abruptly changing to a new policy as a better strategy is found, rather than continuously moving towards an optimal policy.

Over many training runs we find that policies can be categorized into one of the following classes:

- $\pi^0$ : A uniformly random policy (which is the default at the start of training).
- $\pi^1$ : Policy is constant with respect to the state, and moves left with probability 0.5, or up with probability 0.5.

<sup>4</sup>At the start of an episode, there is no previous action, so  $a_{t-1}$  can take on 5 different values

<sup>5</sup>If  $\gamma = 0$  then the behavior of the policy more than one square away from the goal is irrelevant, and for  $\alpha = 0$  the policy only need to be optimal if the goal is in the top left corner.

- $\pi^{2a}$ : Policy is constant with respect to the state, and moves towards the top left corner along a shortest path.
- $\pi^{2b}$ : Same as  $\pi^{2a}$  but choosing a shortest path that passes through the goal on the way to the corner when possible.
- $\pi^3 = \pi^*$ : An optimal policy that moves the agent along a shortest path to the goal square regardless of where the goal is located.

Not all phases are present in every training run, and the dynamics of how policies transition between phases depend strongly on the choices of  $\alpha$  and  $\gamma$ . If  $\alpha = 0$  then the model has only ever seen environments where the goal square is located in the top left corner, and as shown in Abdel Sadek et al. (2025), the model learns to *goal misgeneralize*, and will learn to desire only the top left corner, even when the goal square is placed elsewhere. If  $\alpha = 1$  then there is no pressure to choose the top left corner over any other state, and the model will not learn intermediate phases like  $\pi^1, \pi^{2a}, \pi^{2b}$  that privilege the top left corner. The interesting behavior occurs for intermediate values of  $\alpha$ , where the model goes through a sequence of phases, starting out with  $\pi^1$ , then developing to gradually more complex phases such as  $\pi^{2b}$  and eventually  $\pi^3$ .

A training run with  $\alpha = 0.68, \gamma = 0.99$  is shown in Figure 1. We plot the regret, the difference between the value of the current policy, and that of an optimal policy, as a function of the number of environment steps seen during training. Three chosen points during training are illustrated with depictions of the learned policy in each phase.

With the exception of the default policy  $\pi^0$ , training plateaus in the intermediate suboptimal policies  $\pi^1$  and  $\pi^{2b}$  for a long period during training, and the transitions between them are relatively rapid.

### 3.4.1 Automatic Phase Detection

We will automatically detect when a model lies within a particular phase using an  $L^2$  distance in policy space. Recall that we may identify the space  $\Pi$  of policies in the cheese-in-the-corner model as a product of 3-simplices, since a policy must specify a probability distribution on the set  $\mathcal{A}$  of actions (move up, down, left, right), or a point in the 3-simplex  $\Delta(\mathcal{A}) = \Delta(\{U, D, L, R\})$ , for each state. In other words

$$\Pi = (\Delta(\mathcal{A})^S) \subseteq \mathbb{R}^{4|S|}$$

where the set  $S$  of states has  $11^4 - 11^2 = 14520$  elements. Each phase may be identified as follows.

- Phase 1 corresponds to a specific point in  $\Pi$  – the point associated to the probability distribution  $\pi(U) = \pi(L) = 1/2$  across all states. We may compute the  $L^2$  distance from this point directly.
- Phase 2a corresponds to the intersection of  $\Pi$  with the linear subspace where  $\pi(R) = \pi(D) = 0$  in all states,  $\pi(U) = 0$  in states where the agent is on the top row and  $\pi(L) = 0$  in states where the agent is on the left row. We use the  $L^2$  distance from this subspace.
- Phase 2b corresponds to the subspace of phase 2a where, in addition, if the agent is directly below the goal  $\pi(L) = 0$  and if the agent is directly to the right of the goal  $\pi(U) = 0$ . We again use the  $L^2$  distance from this subspace.
- Phase 3 corresponds to the intersection of  $\Pi$  with the linear subspace where  $\pi(U) = 0$  when the agents vertical position is greater than or equal to that of the goal,  $\pi(D) = 0$  when the agents vertical position is less than or equal to that of the goal,  $\pi(R) = 0$  when the agents horizontal position is greater than or equal to that of the goal and  $\pi(L) = 0$  when the agents horizontal position is less than or equal to that of the goal. We again use the  $L^2$  distance from this subspace.

Given a phase  $P$  let  $d_P$  denote the maximum  $L^2$ -distance from the associated subspace (for instance if  $P$  is a  $D$ -dimensional subspace then  $d_P = \sqrt{4|S| - D}$ ). We let  $\delta = 0.15$  and say that a point  $w \in W$  in parameter space is approximately in phase  $P$  if

$$\min_{\pi \in P} \|\pi_w - \pi\|_2 < \delta d_P.$$

The value of  $\delta$  is chosen to be smaller than the normalized distance between phase 1 and phase 2b in order to detect the transition between those phases. The precise choice of  $\delta = 0.15$  is not critical for the location of the phase transitions, as there is a range over which we could choose  $\delta$  with only minor changes to the corresponding locations of phase transitions (see Section I).

### 3.4.2 Distribution of Phase Transitions

The training trajectory – and therefore the time steps at which phase transitions occur – are random variables, in this section we discuss their empirical distribution. Specifically we will present statistics in eight cases: where the model was trained with  $\alpha = 0.47$  or  $\alpha = 0.68$  and with  $\gamma = 0.9, 0.95, 0.975$  and  $0.99$ . In each hyperparameter case we trained models with these hyperparameters and  $\sim 25$  independent random seeds. In Figure 3 we exhibit the distribution of the training steps at which phase transitions occur as a function of  $\gamma$  for each of the two sampled  $\alpha$ -values. The models transition into phase 1 consistently early in training, the transition from phase 1 to phase 2b depends on  $\gamma$  as we will discuss below.

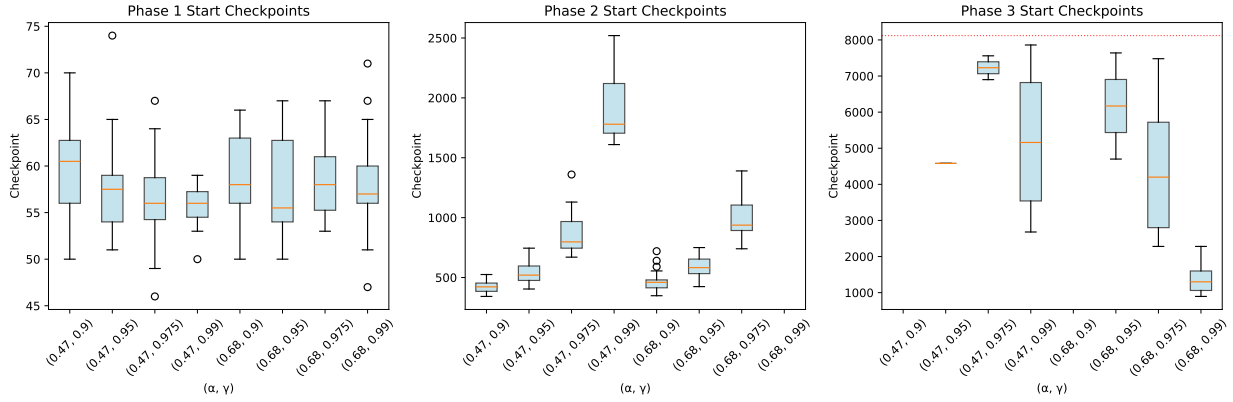


Figure 3: A series of plots illustrating the model transitions into phases  $\pi^1$ ,  $\pi^{2b}$  and  $\pi^3$  respectively, as a function of mixing parameter  $\alpha$  and discount rate  $\gamma$ . We report the number of checkpoints (policy gradient steps) since training began before we enter each phase. The red line in phase 3 represents when training runs were terminated.

We may also study the distribution of the observed phase transitions as a function of  $\alpha$  and  $\gamma$ . We can note the following observations:

1. The number of training steps to transition into  $\pi^1$  is very fast, and unrelated to the choice of  $\alpha, \gamma$  presented.
2. The higher the discount rate, the longer it takes for the model to converge to  $\pi^{2b}$ , if at all. For  $\alpha, \gamma = 0.68, 0.99$ , the policy  $\pi^{2b}$  is never observed, but is skipped entirely, transitioning from  $\pi^1 \rightarrow \pi^3$  directly without visiting  $\pi^{2b}$  first. For  $\alpha, \gamma = 0.68, 0.99$ , during training the policy would sometimes, but not always, skip  $\pi^{2b}$  and transition directly from  $\pi^1 \rightarrow \pi^3$ . This is noted with the \* to indicate we are not measuring the same quantity as the other runs.
3. For  $\alpha, \gamma = 0.47, 0.99$ , some of the runs never reached  $\pi^3$  by the time 5 billion environmental steps had been seen. This means that the collected statistics for this run should be considered with a grain of salt, as early termination of runs that may have converged later are not included in the plot, and this causes a downwards bias in the result.

We can also try to predict the phase transitions based on the hyperparameters with which it was trained, see Section C.

### 3.4.3 LLC Estimates and Phases

Figure 1 shows the LLC estimate and regret across training for a representative model trained with  $\alpha = 0.68$  and  $\gamma = 0.975$ , exhibiting two phase transitions. We present all the estimated LLC curves in Appendix G, Figure 10. We see rapid increases in the LLC estimate at each phase transition, and the increasingly complex phases are associated with increasingly large LLC estimates. We also note a gradual decrease of the LLC estimates in the second halves of phases 2 and 3 as stochastic gradient descent converges to simpler representations of the corresponding local minimum.

Next we discuss the distribution of the LLC estimates within each phase. We performed LLC estimation for 23 independent models trained with  $\alpha = 0.68$  and  $\gamma = 0.975$  – those hyperparameters being selected to maximize the proportion of runs exhibiting two phase transitions. We estimated the LLC at two checkpoints in each of the three phases: Two points at the 1/3 and 2/3 tertiles with respect to the logarithm of the checkpoint number. In Figure 4 we show the distribution of the LLC estimate at these 6 points during training. Using the two internal points within each phase we see mean LLC estimates of 30.92 in phase one (with sample variance  $\hat{\sigma} = 3.38$ ), 106.80 in phase two ( $\hat{\sigma} = 16.19$ ) and 561.52 in phase three ( $\hat{\sigma} = 40.49$ ).

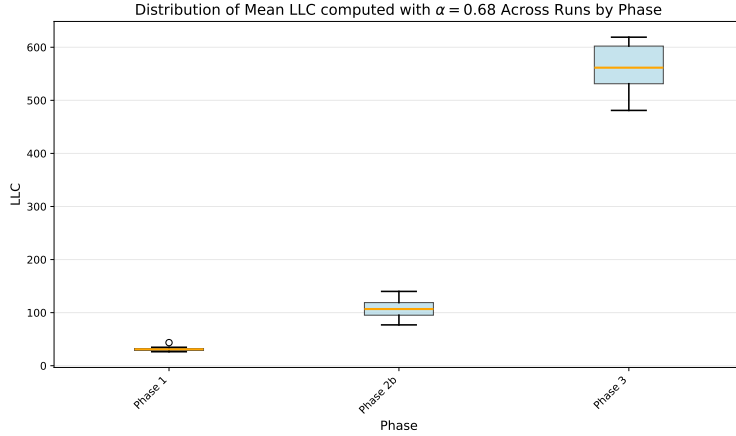


Figure 4: Distribution of average LLC estimates across phases. The LLC has been estimated on distribution with  $\alpha = 0.68$  and  $\gamma = 0.975$ .

### 3.4.4 LLC Estimates with $\alpha = 0$

Let us now examine LLC estimates for the same models as those described in the section above, but estimated with *fixed* values of  $\alpha$  and  $\gamma$  (as described in Remark 3.2 above). We in particular discuss the behavior with  $\alpha = 0$ . In other words during LLC estimation we only consider the behavior of the model in states where the goal is in the top-left corner. Note that in such states we cannot distinguish between phases 2 and 3 by means of the regret anymore: these phases are both optimal and receive zero regret. Nevertheless LLC estimation still allows these phases to be distinguished. We use a fixed value  $\gamma = 0.98$  in this section (and refer to Appendix G for LLC estimate data across models more broadly.)

We again show a representative LLC estimate performed with  $\alpha = 0$  in Figure 5. This estimation was again performed for a representative model trained with  $\alpha = 0.68$  and  $\gamma = 0.975$  exhibiting two phase transitions; the same model used in the previous section. Likewise in Figure 6 we again show the distribution of the LLC estimates at four checkpoints within each phase for 23 independent models trained with  $\alpha = 0.68$  and  $\gamma = 0.975$ . We now see mean LLC estimates of 44.56 in phase one (with sample variance  $\hat{\sigma} = 5.76$ ), 102.54 in phase two ( $\hat{\sigma} = 34.07$ ) and 245.72 in phase three ( $\hat{\sigma} = 149.16$ ).

## 4 Related Work

Measurements of complexity, including those quantifying flatness of a local minimum in the loss landscape have been widely studied for neural networks Hochreiter and Schmidhuber (1997); Keskar et al. (2016); Neyshabur et al. (2017); Dherin et al. (2022). Likewise many authors have explored the idea of simplicity bias in neural networks as an implicit regularization affecting generalization Shah et al. (2020); Teney et al. (2025); Pérez et al. (2018); Morwani et al. (2023). The notion of the loss-complexity tradeoffs and transitions between different solution classes is studied in Singh et al. (2023); Wurgafit et al. (2025); Munn and Wei (2025); Carroll et al. (2025).

The direct study of complexity bias in reinforcement learning specifically has been less explored. The geometry of the reward landscape was explored visually in many examples in Sullivan et al. (2022), which demonstrated the appearance in low-dimensional cross-sections of “cliffs” and “plateaus” in the landscape.

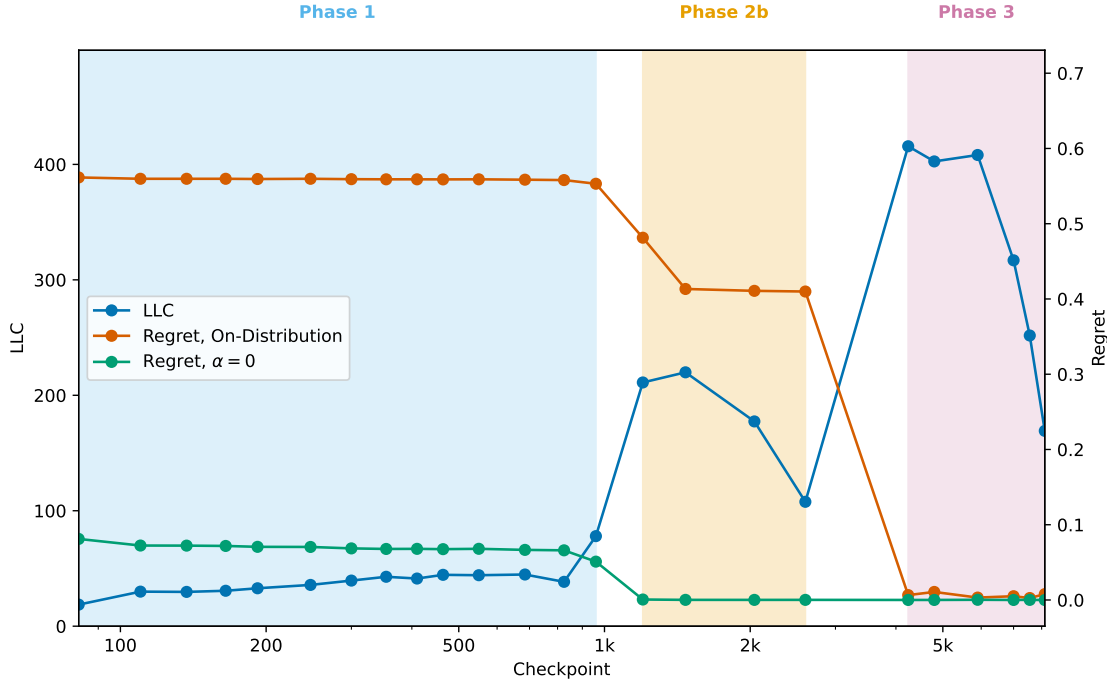


Figure 5: LLC and regret over training for a model trained with  $\alpha = 0.68$  and  $\gamma = 0.975$ . The LLC has been computed with  $\alpha = 0$  and  $\gamma = 0.98$ . We show two regret curves, the orange one with the same  $\alpha$  and  $\gamma$  as was used for training, and the green one with the same  $\alpha$  and  $\gamma$  as was used for LLC estimation.

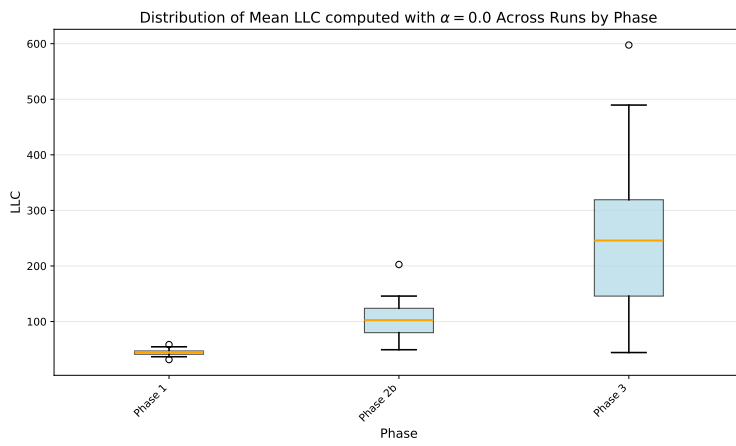


Figure 6: Distribution of average LLC estimates across phases. The LLC has been estimated with  $\alpha = 0$  and  $\gamma = 0.98$ .

The work Boucher et al. (2024) studied the inductive bias introduced by the technique of maximum entropy learning Ziebart et al. (2008) using a range of complexity measures including those that quantified local flatness of a minimum. This idea of flatness specifically as a bias favoring more robust optima was investigated in Lee and Yoon (2025). In Boopathy et al. (2023) the authors studied inductive biases in a range of contexts including reinforcement learning using an information-theoretic measure of complexity. Other authors have applied complexity bias to improve learning performance in reinforcement learning problems You et al. (2025); Lee et al. (2024), while others have studied the generalization of RL agents in grid world similar to the environments considered in this paper (Ramanaukas and Özgür Şimşek, 2023; Abdel Sadek et al., 2025).

The approach taken in this paper of characterizing complexity of a point in parameter space in terms of the local geometry of the regret function is complementary to work that characterizes the complexity of the function class represented by parameter space (including those inspired by Rademacher complexity and Vapnik–Chernovenkis dimension in supervised learning). This latter approach is taken for reinforcement learning in the complexity measures developed in Jiang et al. (2017); Russo and Van Roy (2013). The *decision-estimation coefficient* defined in Foster et al. (2021) also follows this approach but with a structure that permits localized estimation near a point in parameter space.

We lastly mention some of the theoretical literature on the dynamics of reinforcement learning. The dynamics under policy gradient learning was studied in an illustrative model for reinforcement learning in Patel et al. (2025). The connection between complexity and stagewise development has recently been explored in the supervised learning case, particularly for large language models Wei et al. (2022a); Wang et al. (2024); Chen et al. (2024a). Finally in the neuroscience literature, it has been demonstrated that stagewise development also occurs during reinforcement learning in biology Liebana et al. (2025).

## 5 Discussion

### 5.1 Off-policy learning

A subtlety in relating the generalized posterior to practical RL training is the appearance of the sequence of behavior parameters  $w_1, \dots, w_n$  in the dataset  $D_n = \{(w_i, \tau_i)\}_{i=1}^n$ . From a practical off-policy RL perspective, there is a standard answer to “where do the  $w_i$  come from?”: they are the (possibly stale) policy parameters that were used to *collect* the experience currently being used for learning.

Concretely, modern off-policy RL algorithms decouple data collection from parameter updates by maintaining a replay buffer (or a distributed set of actors) containing trajectories or transitions generated under a sequence of behavior policies. If at training time-step  $k$  the learner has parameters  $w^{(k)}$  and collects a batch of trajectories  $\tau_1^{(k)}, \dots, \tau_{B_k}^{(k)} \sim q_{w^{(k)}}$ , then the accumulated dataset over training naturally has the form

$$\{(w^{(k)}, \tau_j^{(k)}) : k \leq K, 1 \leq j \leq B_k\},$$

i.e. it is a union of samples drawn under earlier iterates of the same SGD process.<sup>6</sup> Thus, even though our theory allows an arbitrary sequence  $(w_i)_{i=1}^n$ , the “canonical” source of such a sequence in practice is simply *the learning algorithm itself*, via checkpoints or lagged actors.

Recall that the RL objective is to maximize expected return  $R(w)$ , equivalently to minimize regret  $G(w) = R_{\max} - R(w)$  so  $\nabla_w R(w) = -\nabla_w G(w)$ . The score-function identity gives

$$\nabla_w R(w) = \nabla_w \mathbb{E}_{\tau \sim q_w} [r(\tau)] = \mathbb{E}_{\tau \sim q_w} [r(\tau) \nabla_w \log q_w(\tau)]. \quad (11)$$

Using the factorization  $q_w(\tau) = q_{\text{env}}(\tau) \prod_{t=1}^T \pi_w(a_t | o_{t-1})$  we obtain

$$\nabla_w \log q_w(\tau) = \sum_{t=1}^T \nabla_w \log \pi_w(a_t | o_{t-1}), \quad (12)$$

<sup>6</sup>In distributed actor–learner architectures one should interpret  $w^{(k)}$  as the parameters on the actor at the moment of rollout, which are typically a lagged copy of the learner parameters.

which is the usual REINFORCE structure. Finally, by the standard “reward-to-go” (causality) argument one may replace the full return  $r(\tau)$  in (11) by  $r(\tau_{\geq t})$  at time  $t$ , yielding an equivalent estimator

$$\nabla_w R(w) = \mathbb{E}_{\tau \sim q_w} \left[ \sum_{t=1}^T r(\tau_{\geq t}) \nabla_w \log \pi_w(a_t | o_{t-1}) \right], \quad (13)$$

which matches the on-policy training rule used in this paper (cf. (9)).

Now consider the off-policy setting where trajectories are generated under behavior policies  $\pi_{w_i}$  and we wish to improve a *target* policy  $\pi_w$ . Applying the same change-of-measure identity used above (11) becomes

$$\nabla_w R(w) = \mathbb{E}_{\tau \sim q_{w_i}} \left[ \frac{q_w(\tau)}{q_{w_i}(\tau)} r(\tau) \nabla_w \log q_w(\tau) \right], \quad (14)$$

and substituting (12) and the reward-to-go form yields the canonical off-policy REINFORCE estimator

$$\nabla_w R(w) = \mathbb{E}_{\tau \sim q_{w_i}} \left[ \frac{q_w(\tau)}{q_{w_i}(\tau)} \sum_{t=1}^T r(\tau_{\geq t}) \nabla_w \log \pi_w(a_t | o_{t-1}) \right]. \quad (15)$$

The connection to our empirical regret estimator is immediate. Differentiating  $G_n$  gives

$$\begin{aligned} \nabla_w G_n(w) &= \frac{1}{n} \sum_{i=1}^n \frac{q_w(\tau_i)}{q_{w_i}(\tau_i)} g(\tau_i) \nabla_w \log q_w(\tau_i) \\ &= \frac{1}{n} \sum_{i=1}^n \frac{q_w(\tau_i)}{q_{w_i}(\tau_i)} \sum_{t=1}^{T_i} g(\tau_i) \nabla_w \log \pi_w(a_{i,t} | o_{i,t-1}), \end{aligned} \quad (16)$$

and replacing  $g(\tau_i)$  by its reward-to-go form yields the trajectory-sampled analogue of (15) (up to the overall sign corresponding to maximizing return vs. minimizing regret). Thus, stochastic gradient descent on  $G_n$  corresponds to an off-policy REINFORCE-style update, while the generalized posterior is the Gibbs distribution associated to the same empirical objective.

## 5.2 Relation between Bayesian learning and SGD

In the theoretical part of this paper (Section 2) we have given a description of the Bayesian learning process in RL in terms of an evolving tradeoff between regret and complexity, as made precise by the free energy formula. This predicts *Bayesian phase transitions* as the generalized posterior  $p(w|D_n) \propto \exp(-nG_n(w))\phi(w)$  shifts its concentration between local minima of the population regret  $G$ . Here  $n$  denotes the number of trajectories “seen” by the learner and incorporated into the posterior update.

In the experimental part of the paper (Section 3) we studied the training process of a deep RL agent by SGD. The optimization draws for each gradient step batches of  $B$  trajectories and the gradient estimator in (9) is essentially  $\nabla_w G_n(w)$  with  $n = B$ . After  $S$  steps of gradient descent, information from  $BS$  trajectories have influenced the current parameter.

To attempt to line these two learning processes up as much as possible, we can take the sequence of behavioral parameters of Section 5.1 to be  $w_1, \dots, w_1, \dots, w_S, \dots, w_S$  where  $w_i$  is the  $i$ th step of gradient descent and each parameter is repeated  $B$  times, and take the  $\tau_i$  to be the contents of mini-batches sampled during SGD. Thus in some sense  $D_n$  is the set of trajectories seen so far by SGD. But even then the relation of  $p(w|D_n)$  with the distribution of SGD endpoints (with initialization and sampling providing the randomness) is obscure. This is the open question, mentioned in the introduction, of the relation between posterior concentration and SGD dynamics.

In this paper we take a more local perspective. The *Bayesian antecedent hypothesis* proposed in Chen et al. (2024b) claims that dynamical transitions (such as the ones observed in our experiments, where the optimization trajectory moves from plateau to plateau via sudden drops) are the “shadow” of Bayesian phase transitions in the following sense: each plateau corresponds to a region of parameter space around some local minima of the regret (a “phase”) and if there is a dynamical transition between two plateaus, there

should be a Bayesian phase transition (the Bayesian antecedent) in which the posterior shifts concentration between the corresponding regions.

The existence of such a Bayesian antecedent does make a prediction: the LLC should rise during dynamical transitions. This was observed in Chen et al. (2024b) for supervised learning, and we see similar results here in the setting of reinforcement learning. In our experiments we can see that the estimate of the LLC coincides with a naïve assessment of policy complexity and phase transitions correspond to transitions from simpler but less optimal policies to policies that are more complex but more optimal. In the Bayesian setting singular learning theory, and the LLC in particular, provides a rigorous formalization of the notion of *complexity* of learning for deep RL models. Our empirical results are evidence that this notion of complexity is also applicable in the context of stochastic optimization.

### 5.3 Relevance to alignment

The results of Section 2 have implications for AI alignment. There is a subtle but important distinction between the prevailing (albeit implicit and underdeveloped) view on how policies of deep RL agents develop over training, and the SLT-informed view that this paper provides:

- **Standard view:** policies earlier in training are qualitatively similar to policies later in training, which are obtained by *refining* and *adding to* earlier policies. If we haven’t converged to an optimal policy it’s not for some fundamental reason, it’s just a flaw in the optimization process or lack of compute.
- **SLT-informed view:** policies earlier in training can be qualitatively different to policies later in training and phase transitions can involve fundamental changes in the underlying algorithm. If we haven’t converged to an optimal policy, it may be because it is being screened by a lower complexity solution that is Bayes optimal at the given dataset size.

By the logic of Section 2.7 a lower complexity solution can be preferred to a lower regret solution if

$$\delta\lambda > \frac{n}{\log n} \delta G. \quad (17)$$

In cases where there are any theoretical guarantees at all, alignment assumes “near enough” convergence to an optimal policy, which is safe (Hadfield-Menell et al., 2024; Kosoy, 2023). Let  $\delta G$  be the allowed gap to this optimal safe policy and let us refer to any policy with higher regret as “misaligned”. We analogize Bayesian learning to SGD training, under some relation between dataset size  $n$  and the number of trajectories seen over training  $BS$  as in Section 5.2, and let  $C = n / \log n$  be determined by the available compute. Then by (17) the generalized posterior can prefer a local minimum of  $G$  which is *misaligned but simpler* than the optimal (aligned) policy by more than  $C\delta G$  (Pepin Lehalleur et al., 2025).

Goal misgeneralization (Langosco et al., 2022; Abdel Sadek et al., 2025) is arguably an example of this phenomena. Indeed Langosco et al. (2022, §2.2) give inductive bias towards simplicity as their main suggestion for the origin of goal misgeneralization. Our experimental setting is a simplified form of the one studied in that work, and in the training run presented in Figure 1 if training had stopped at checkpoint 2k, the policy would be “misaligned” in the sense that the designer of the environment might have intended a trained agent to seek the cheese (this is after all the optimal policy).

Similar logic applies to reward hacking in RLHF (Lambert, 2026). Reward models trained on human preference data may learn simple correlations (e.g., “longer responses are better” (Shen et al., 2023) or “lists are preferred” (Zhang et al., 2025)) rather than complex representations of genuine quality (Gao et al., 2022). If the simpler pattern achieves comparable loss on the preference dataset, the free energy formula (for supervised learning) predicts it will be favored during training. When this reward model is used to train the policy, these biases are amplified and also interact with the simplicity bias of the RL training process.

There is also a connection to instrumental convergence (Omohundro, 2018; Bostrom, 2014). Consider an RL agent trained on a large set of diverse environments. If the environment is easily recognizable, the optimal policy  $\pi^*$  will detect the environment and then act in a way tailored to that specific task. However, acquiring resources or control of the environment may be a commonly represented pattern in successful policies across a broad range of environment, and *these behaviors may be simpler to represent* than a large number of tailored

policies. Hence a parameter which parametrizes an *instrumentally convergent* policy  $\pi^{\text{inst}}$  might be preferred by the posterior even if it is higher regret than  $\pi^*$ .

## 6 Conclusion

We have extended singular learning theory to deep reinforcement learning, proving that the concentration of the generalized posterior over parameters for policies is governed by the local learning coefficient – an invariant of the geometry of the regret function (Theorem 2.3). This provides a precise theoretical foundation for the intuitive concept of simplicity bias in deep RL: the free energy formula characterizes Bayesian learning as an evolving tradeoff between regret and complexity, predicting that phase transitions should proceed from simple, high-regret policies to complex, low-regret policies.

Our main theoretical insight is that *a more optimal policy is not always more optimal from a Bayesian perspective*. Depending on the number of trajectories seen, a Bayesian learner may prefer a simpler policy with higher regret over a complex policy with lower regret. This is characterized precisely by the critical dataset size  $n^*$  at which the posterior shifts concentration between competing solutions. One practical implication is that for any finite training process, simpler but less aligned policies may be favored – a phenomenon we connect to goal misgeneralization, reward hacking, and potentially instrumental convergence (Section 5.3).

Our empirical results validate the theory’s predictions. In a gridworld environment exhibiting stagewise learning, we observe “opposing staircases” where phase transitions manifest as rapid decreases in regret accompanied by rapid increases in the LLC. Notably, the LLC detects the transition between phases 2b and 3 even when estimated on states where both policies achieve identical regret, suggesting it captures changes in the underlying algorithm rather than merely performance. This demonstrates that the geometry of the regret function reveals structure in the learning process that is invisible to behavioral metrics alone.

The extension of singular learning theory to reinforcement learning opens several directions for future work. First, carefully quantifying how Bayesian posterior concentration relates to SGD dynamics remains an important open problem. Second, the techniques developed here – and related methods for measuring and manipulating model structure (Wang et al., 2025; Baker et al., 2025; Kreer et al., 2025) – should be applicable to alignment-relevant phenomena in more complex reinforcement learning settings including RL training of large language models. Given the centrality of reinforcement learning to the training of frontier AI systems, we believe that understanding and measuring complexity-regret tradeoffs is an important direction for AI safety research.

## Acknowledgements

We would like to thank Edmund Lau for his involvement in the early stages of this project and for many helpful suggestions. We are very grateful to Marcus Hutter and Vanessa Kosoy for productive conversations on the topic of this paper during the Mathematical Science of AI Safety focus period at SMRI. We are also grateful to Rohan Hitchcock for sharing the argument used in the proof of Lemma E.31 and to Shaowei Lin for providing guidance concerning the control as influence literature. Finally we would like to thank Zach Furman, Philipp Alexander Kreer and Rumi Salazar for their feedback on an earlier draft.

This project is funded by the Advanced Research + Invention Agency (ARIA).

## References

- K. Abdel Sadek, M. Farrugia-Roberts, H. Erlebach, C. S. de Witt, D. Krueger, U. Anwar, and M. D. Dennis. Mitigating goal misgeneralization via minimax regret. In *Reinforcement Learning Conference*, 2025.
- U. Anwar, A. Saparov, J. Rando, D. Paleka, M. Turpin, P. Hase, E. S. Lubana, E. Jenner, S. Casper, O. Sourbut, B. L. Edelman, Z. Zhang, M. Günther, A. Korinek, J. Hernandez-Orallo, L. Hammond, E. Bigelow, A. Pan, L. Langosco, T. Korbak, H. Zhang, R. Zhong, S. O. Eigeartaigh, G. Recchia, G. Corsi, A. Chan, M. Anderljung, L. Edwards, A. Petrov, C. S. de Witt, S. R. Motwan, Y. Bengio, D. Chen, P. H. S. Torr,

S. Albanie, T. Maharaj, J. Foerster, F. Tramer, H. He, A. Kasirzadeh, Y. Choi, and D. Krueger. Foundational challenges in assuring alignment and safety of large language models, 2024. URL <https://arxiv.org/abs/2404.09932>.

G. Baker, G. Wang, J. Hoogland, and D. Murfet. Structural inference: Interpreting small language models with susceptibilities. *arXiv preprint arXiv:2504.18274*, 2025.

V. Balasubramanian. Statistical inference, occam’s razor, and statistical mechanics on the space of probability distributions. *Neural Computation*, 9(2):349–368, 02 1997. ISSN 0899-7667. doi: 10.1162/neco.1997.9.2.349. URL <https://doi.org/10.1162/neco.1997.9.2.349>.

P. G. Bissiri, C. C. Holmes, and S. G. Walker. A general framework for updating belief distributions. *Journal of the Royal Statistical Society: Series B (Statistical Methodology)*, 78(5):1103–1130, 2016. doi: <https://doi.org/10.1111/rssb.12158>. URL <https://rss.onlinelibrary.wiley.com/doi/abs/10.1111/rssb.12158>.

A. Boopathy, K. Liu, J. Hwang, S. Ge, A. Mohammedsaleh, and I. R. Fiete. Model-agnostic measure of generalization difficulty. In *International Conference on Machine Learning*, 2023. URL <https://api.semanticscholar.org/CorpusID:258436843>.

N. Bostrom. *Superintelligence: Paths, Dangers, Strategies*. Oxford University Press, 2014.

R. H. Boucher, O. Semeraro, and L. Mathelin. Evidence on the regularisation properties of maximum-entropy reinforcement learning. In *International Conference on Optimization and Learning*, pages 123–139. Springer, 2024.

N. Brosse, A. Durmus, and E. Moulines. The promises and pitfalls of stochastic gradient langevin dynamics. *Advances in Neural Information Processing Systems*, 31, 2018.

L. Carroll, J. Hoogland, M. Farrugia-Roberts, and D. Murfet. Dynamics of transient structure in in-context linear regression transformers. *arXiv preprint arXiv:2501.17745*, 2025.

A. Chen, R. Shwartz-Ziv, K. Cho, M. L. Leavitt, and N. Saphra. Sudden drops in the loss: Syntax acquisition, phase transitions, and simplicity bias in MLMs. In *The Twelfth International Conference on Learning Representations*, 2024a. URL <https://openreview.net/forum?id=MO5PiKHELW>.

Z. Chen, E. Lau, J. Mendel, S. Wei, and D. Murfet. Dynamical versus Bayesian phase transitions in a toy model of superposition, 2024b. URL <https://openreview.net/forum?id=uf5EAQmkrN>.

J. Clift, D. Doryn, D. Murfet, and J. Wallbridge. Logic and the 2-simplicial transformer. In *International Conference on Learning Representations*, 2020. URL <https://openreview.net/forum?id=rkecJ6VFvr>.

B. Dherin, M. Munn, M. Rosca, and D. G. T. Barrett. Why neural networks find simple solutions: the many regularizers of geometric complexity. *CoRR*, abs/2209.13083, 2022. URL <https://doi.org/10.48550/arXiv.2209.13083>.

L. Espeholt, H. Soyer, R. Munos, K. Simonyan, V. Mnih, T. Ward, Y. Doron, V. Firoiu, T. Harley, I. Dunning, S. Legg, and K. Kavukcuoglu. Impala: Scalable distributed deep-rl with importance weighted actor-learner architectures, 2018. URL <https://arxiv.org/abs/1802.01561>.

D. J. Foster, S. M. Kakade, J. Qian, and A. Rakhlin. The statistical complexity of interactive decision making. *arXiv preprint arXiv:2112.13487*, 2021.

L. Gao, J. Schulman, and J. Hilton. Scaling laws for reward model overoptimization, 2022. URL <https://arxiv.org/abs/2210.10760>.

D. Hadfield-Menell, A. Dragan, P. Abbeel, and S. Russell. Cooperative inverse reinforcement learning, 2024. URL <https://arxiv.org/abs/1606.03137>.

J. Hartigan. Asymptotic normality of posterior distributions. In *Bayes theory*, pages 107–118. Springer, 1983.

H. Hironaka. Resolution of singularities of an algebraic variety over a field of characteristic zero: I. *Annals of Mathematics*, 79(2):109–203, 1964.

R. Hitchcock and J. Hoogland. From global to local: A scalable benchmark for local posterior sampling. *arXiv preprint 2507.21449*, 2025.

S. Hochreiter and J. Schmidhuber. Flat minima. *Neural Computation*, 9:1–42, 1997. URL <https://api.semanticscholar.org/CorpusID:733161>.

J. Hoogland, G. Wang, M. Farrugia-Roberts, L. Carroll, S. Wei, and D. Murfet. Loss landscape degeneracy drives stagewise development in transformers, 2025. URL <https://arxiv.org/abs/2402.02364>.

N. Jiang, A. Krishnamurthy, A. Agarwal, J. Langford, and R. E. Schapire. Contextual decision processes with low Bellman rank are PAC-learnable. In *International Conference on Machine Learning*, pages 1704–1713. PMLR, 2017.

R. E. Kalman. A new approach to linear filtering and prediction problems. *Transactions of the ASME, Journal of Basic Engineering*, 82:35–45, 1960.

N. S. Keskar, D. Mudigere, J. Nocedal, M. Smelyanskiy, and P. T. P. Tang. On large-batch training for deep learning: Generalization gap and sharp minima. *ArXiv*, abs/1609.04836, 2016. URL <https://api.semanticscholar.org/CorpusID:5834589>.

V. Kosoy. The learning-theoretic agenda: Status 2023. LessWrong, Apr. 2023. URL <https://www.lesswrong.com/posts/ZwshvqiqCvXPsZEct/the-learning-theoretic-agenda-status-2023>. Accessed: 2026-01-08.

P. A. Kreer, W. Wu, M. Adam, Z. Furman, and J. Hoogland. Bayesian influence functions for Hessian-free data attribution. *ArXiv*, abs/2509.26544, 2025. URL <https://api.semanticscholar.org/CorpusID:281681466>.

N. Lambert. Reinforcement learning from human feedback, 2026. URL <https://arxiv.org/abs/2504.12501>.

L. L. D. Langosco, J. Koch, L. D. Sharkey, J. Pfau, and D. Krueger. Goal misgeneralization in deep reinforcement learning. In K. Chaudhuri, S. Jegelka, L. Song, C. Szepesvari, G. Niu, and S. Sabato, editors, *Proceedings of the 39th International Conference on Machine Learning*, volume 162 of *Proceedings of Machine Learning Research*, pages 12004–12019. PMLR, 17–23 Jul 2022. URL <https://proceedings.mlr.press/v162/langosco22a.html>.

E. Lau, Z. Furman, G. Wang, D. Murfet, and S. Wei. The local learning coefficient: A singularity-aware complexity measure. In *The 28th International Conference on Artificial Intelligence and Statistics*, 2025. URL <https://openreview.net/forum?id=1av51Z1suL>.

H. Lee, D. Hwang, D. Kim, H. Kim, J. J. Tai, K. Subramanian, P. R. Wurman, J. Choo, P. Stone, and T. Seno. SimBa: Simplicity bias for scaling up parameters in deep reinforcement learning. *ArXiv*, abs/2410.09754, 2024. URL <https://api.semanticscholar.org/CorpusID:273346233>.

H. K. Lee and S. W. Yoon. Flat reward in policy parameter space implies robust reinforcement learning. In *The Thirteenth International Conference on Learning Representations*, 2025. URL <https://openreview.net/forum?id=4Oa03GjP7k>.

S. Levine. Reinforcement learning and control as probabilistic inference: Tutorial and review. *arXiv preprint arXiv:1805.00909*, 2018.

C. Li, C. Chen, D. Carlson, and L. Carin. Preconditioned stochastic gradient langevin dynamics for deep neural networks, 2015. URL <https://arxiv.org/abs/1512.07666>.

S. Liebana, A. Laffere, C. Toschi, L. Schilling, J. Moretti, J. Podlaski, M. Fritsche, P. Zatka-Haas, Y. Li, R. Bogacz, et al. Dopamine encodes deep network teaching signals for individual learning trajectories. *Cell*, 188(4), 2025.

T. McGrath, A. Kapishnikov, N. Tomašev, A. Pearce, M. Wattenberg, D. Hassabis, B. Kim, U. Paquet, and V. Kramnik. Acquisition of chess knowledge in alphazero. *Proceedings of the National Academy of Sciences*, 119(47), 2022. doi: 10.1073/pnas.2206625119.

U. Mini, P. Grietzer, M. Sharma, A. Meek, M. MacDiarmid, and A. M. Turner. Understanding and controlling a maze-solving policy network. *arXiv preprint arXiv:2310.08043*, 2023.

D. Morwani, J. Batra, P. Jain, and P. Netrapalli. Simplicity bias in 1-hidden layer neural networks. *ArXiv*, abs/2302.00457, 2023. URL <https://api.semanticscholar.org/CorpusID:256459772>.

M. Munn and S. Wei. A Bayesian model selection criterion for selecting pretraining checkpoints. In *Forty-second International Conference on Machine Learning*, 2025. URL <https://openreview.net/forum?id=fEjktWQ5Am>.

S. Nagayasu and S. Watanbe. Asymptotic behavior of free energy when optimal probability distribution is not unique. *Neurocomputing*, 500:528–536, 2022.

B. Neyshabur, S. Bhojanapalli, D. McAllester, and N. Srebro. Exploring generalization in deep learning. *Advances in neural information processing systems*, 30, 2017.

S. M. Omohundro. The basic AI drives. In *Artificial Intelligence Safety and Security*, pages 47–55. Chapman and Hall/CRC, July 2018. doi: 10.1201/9781351251389-3.

N. Patel, S. Lee, S. Sarao Mannelli, S. Goldt, and A. Saxe. Rl perceptron: Generalization dynamics of policy learning in high dimensions. *Physical Review X*, 15(2):021051, 2025.

S. Pepin Lehalleur, J. Hoogland, M. Farrugia-Roberts, S. Wei, A. G. Oldenziel, G. Wang, L. Carroll, and D. Murfet. You are what you eat—AI alignment requires understanding how data shapes structure and generalisation. *arXiv preprint arXiv:2502.05475*, 2025.

G. V. Pérez, C. Q. Camargo, and A. Louis. Deep learning generalizes because the parameter-function map is biased towards simple functions. *ArXiv*, abs/1805.08522, 2018. URL <https://arxiv.org/pdf/1805.08522.pdf>.

K. Ramanauskas and Özgür Şimşek. Colour versus shape goal misgeneralization in reinforcement learning: A case study, 2023. URL <https://arxiv.org/abs/2312.03762>.

G. O. Roberts and R. L. Tweedie. Exponential convergence of Langevin distributions and their discrete approximations. *Bernoulli*, 2(4):341–363, 1996.

D. Russo and B. Van Roy. Eluder dimension and the sample complexity of optimistic exploration. *Advances in Neural Information Processing Systems*, 26, 2013.

G. Schwarz. Estimating the Dimension of a Model. *The Annals of Statistics*, 6(2):461 – 464, 1978. doi: 10.1214/aos/1176344136. URL <https://doi.org/10.1214/aos/1176344136>.

H. S. Seung, H. Sompolinsky, and N. Tishby. Statistical mechanics of learning from examples. *Physical review A*, 45(8):6056, 1992.

H. Shah, K. Tamuly, A. Raghunathan, P. Jain, and P. Netrapalli. The pitfalls of simplicity bias in neural networks. In H. Larochelle, M. Ranzato, R. Hadsell, M. Balcan, and H. Lin, editors, *Advances in Neural Information Processing Systems 33: Annual Conference on Neural Information Processing Systems 2020, NeurIPS 2020, December 6-12, 2020, virtual*, 2020. URL <https://proceedings.neurips.cc/paper/2020/hash/6cfe0e6127fa25df2a0ef2ae1067d915-Abstract.html>.

W. Shen, R. Zheng, W. Zhan, J. Zhao, S. Dou, T. Gui, Q. Zhang, and X. Huang. Loose lips sink ships: Mitigating length bias in reinforcement learning from human feedback, 2023. URL <https://arxiv.org/abs/2310.05199>.

A. K. Singh, S. C. Y. Chan, T. Moskovitz, E. Grant, A. M. Saxe, and F. Hill. The transient nature of emergent in-context learning in transformers. *ArXiv*, abs/2311.08360, 2023. URL <https://api.semanticscholar.org/CorpusID:265157721>.

R. Sullivan, J. K. Terry, B. Black, and J. P. Dickerson. Cliff diving: Exploring reward surfaces in reinforcement learning environments. In K. Chaudhuri, S. Jegelka, L. Song, C. Szepesvari, G. Niu, and S. Sabato, editors, *Proceedings of the 39th International Conference on Machine Learning*, volume 162 of *Proceedings of Machine Learning Research*, pages 20744–20776. PMLR, 7 2022. URL <https://proceedings.mlr.press/v162/sullivan22a.html>.

Y. W. Teh, A. H. Thiery, and S. J. Vollmer. Consistency and fluctuations for stochastic gradient langevin dynamics. *The Journal of Machine Learning Research*, 17(1):193–225, 2016.

D. Teney, L. Jiang, F. Gogianu, and E. Abbasnejad. Do we always need the simplicity bias? looking for optimal inductive biases in the wild. In *Proceedings of the Computer Vision and Pattern Recognition Conference*, pages 79–90, 2025.

E. Todorov. General duality between optimal control and estimation. In *2008 47th IEEE Conference on Decision and Control*, pages 4286–4292, 2008. doi: 10.1109/CDC.2008.4739438.

M. Toussaint and A. Storkey. Probabilistic inference for solving discrete and continuous state Markov decision processes. In *Proceedings of the 23rd International Conference on Machine Learning*, pages 945–952, 2006.

G. Wang, M. Farrugia-Roberts, J. Hoogland, L. Carroll, S. Wei, and D. Murfet. Loss landscape geometry reveals stagewise development of transformers. In *High-dimensional Learning Dynamics 2024: The Emergence of Structure and Reasoning*, 2024. URL <https://openreview.net/forum?id=2JabyZjM5H>.

G. Wang, J. Hoogland, S. van Wingerden, Z. Furman, and D. Murfet. Differentiation and specialization of attention heads via the refined local learning coefficient. In *The Thirteenth International Conference on Learning Representations*, 2025. URL <https://openreview.net/forum?id=SUc1UOWndp>.

S. Watanabe. Almost all learning machines are singular. In *2007 IEEE Symposium on Foundations of Computational Intelligence*, pages 383–388. IEEE, 2007.

S. Watanabe. *Algebraic geometry and statistical learning theory*, volume 25 of *Cambridge Monographs on Applied and Computational Mathematics*. Cambridge University Press, 2009.

S. Watanabe. Asymptotic learning curve and renormalizable condition in statistical learning theory. In *Journal of Physics: Conference Series*, volume 233, page 012014. IOP Publishing, 2010.

S. Watanabe. A widely applicable Bayesian information criterion. *The Journal of Machine Learning Research*, 14(1):867–897, 2013.

S. Watanabe. *Mathematical theory of Bayesian statistics*. Chapman and Hall/CRC, 2018.

J. Wei, Y. Tay, R. Bommasani, C. Raffel, B. Zoph, S. Borgeaud, D. Yogatama, M. Bosma, D. Zhou, D. Metzler, E. H. Chi, T. Hashimoto, O. Vinyals, P. Liang, J. Dean, and W. Fedus. Emergent abilities of large language models. *Transactions on Machine Learning Research*, 2022a. ISSN 2835-8856. URL <https://openreview.net/forum?id=yzkSU5zdwD>. Survey Certification.

S. Wei, D. Murfet, M. Gong, H. Li, J. Gell-Redman, and T. Quella. Deep learning is singular, and that's good. *IEEE Transactions on Neural Networks and Learning Systems*, 34(12):10473–10486, 2022b.

M. Welling and Y. W. Teh. Bayesian learning via stochastic gradient Langevin dynamics. In *Proceedings of the 28th international conference on machine learning (ICML-11)*, pages 681–688, 2011.

D. Wurgafit, E. S. Lubana, C. F. Park, H. Tanaka, G. Reddy, and N. D. Goodman. In-context learning strategies emerge rationally. *ArXiv*, abs/2506.17859, 2025. URL <https://api.semanticscholar.org/CorpusID:279999158>.

B. You, C. Wang, and H. Liu. Trajectory entropy reinforcement learning for predictable and robust control. *ArXiv*, abs/2505.04193, 2025. URL <https://api.semanticscholar.org/CorpusId:278367880>.

T. Zhang. From  $\epsilon$ -entropy to KL-entropy: Analysis of minimum information complexity density estimation. *The Annals of Statistics*, pages 2180–2210, 2006.

X. Zhang, W. Xiong, L. Chen, T. Zhou, H. Huang, and T. Zhang. From lists to emojis: How format bias affects model alignment, 2025. URL <https://arxiv.org/abs/2409.11704>.

B. D. Ziebart, A. L. Maas, J. A. Bagnell, A. K. Dey, et al. Maximum entropy inverse reinforcement learning. In *Aaai*, volume 8, pages 1433–1438. Chicago, IL, USA, 2008.

## A Outlook

In this appendix we give a discussion of some further directions that the introduction of singular learning theory to the reinforcement learning context allows one to pursue.

### Weight-Refined LLCs

It was demonstrated in Wang et al. (2025) that one can detect the development of structure in parameter space during training by studying what they refer to as *weight-refined* LLCs – LLCs for the restriction of the loss function to a subspace of parameter space. They study transformer models and detect differentiation of attention heads during training using this method, and these techniques are also applicable in the reinforcement learning context. By estimating refined LLCs for, for instance, individual layers of the deep neural network in deep reinforcement learning we may detect development of internal structure that is not visible from looking at the policy alone.

### Susceptibilities

The techniques of singular learning theory may be applied to the expectation values of more general observables with respect to the Gibbs posterior. What's more, if the loss function one considers depends on a hyperparameter (in our setting we saw the dependence of the regret on the hyperparameters  $\alpha, \gamma$ ) one can study the infinitesimal change in these expectation values with respect to the variation of these hyperparameters. In Baker et al. (2025) the authors study exactly this setting: their *susceptibilities* correspond to the variation of weight-refined LLCs under infinitesimal perturbations of the data distribution. In the reinforcement learning setting one can do the same thing, where one varies either the reward function of the Markov problem or the initial state distribution.

### Environment Complexity

By enhancing our toy model slightly one could explore the ability of the LLC estimator to detect out-of-distribution generalization, meaning here performance in classes of states not seen during training. For a simple example consider the extension of the model presented here to maze environments (as in the original cheese-in-the-corner example presented in Abdel Sadek et al. (2025)). One can allow the distribution of initial states used during training and LLC estimation to differ, as we did in Section 3.4.4, but now changes in the LLC may detect changes in performance in out-of-distribution states.

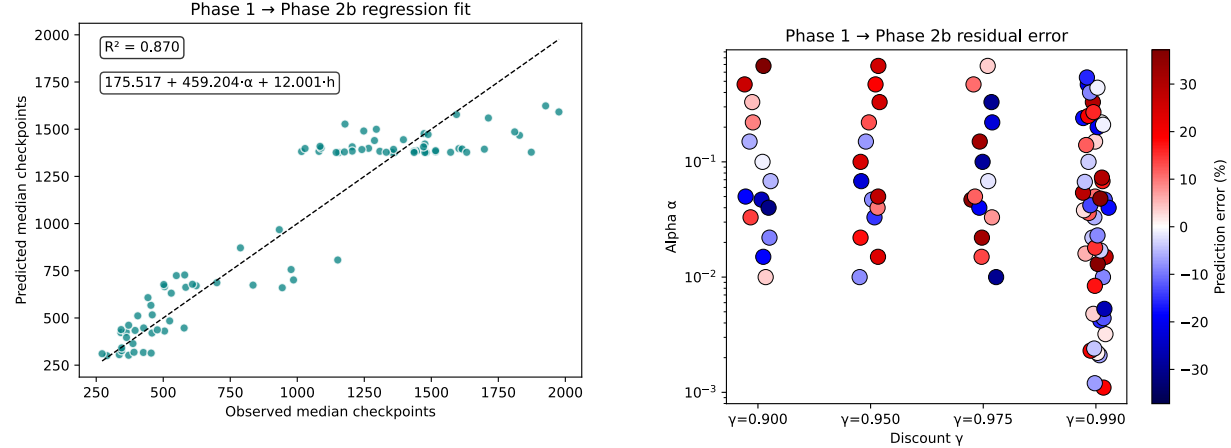
### Stochastic Transitions

Finally we discuss a theoretical question. To what extent is it possible to relax the assumption that the transition functions of the Markov problem are deterministic? We may immediately relax it a little to the condition given in Assumption E.16 – that optimal policies may obtain optimal reward with probability one – but new techniques will be required to go beyond this. Note that this condition is analogous to a hierarchy of assumptions that appear in Watanabe's work in the context of distribution learning from iid data (essential uniqueness, renormalizability as in Watanabe (2010) or the relative finite variance condition in Watanabe (2018)). An approach to generalize beyond this might build on the non-essentially-unique example of Nagayasu and Watanabe (2022), in which a more significant term appears in the free energy.

## B LLC Estimation

Here we include additional details relevant to Section 3.3.

When running the LLC estimation, we run 5 SGLD regret chains, with 6000 steps per chain and 4800 levels per step. We use a localization strength of 200 (so  $\sigma^2 = 1/200$ ),  $n\beta$  of 1000, learning rate of  $10^{-6}$ . When selecting the SGLD hyperparameters we aim to make the SGLD chains long enough that the mean chain regrets converge while avoiding the following pitfalls.



(a) A scatter plot of all training runs with the number of gradient steps for the transition  $\pi^1 \rightarrow \pi^{2b}$ , v.s. the predicted number according to the equation found via linear regression. For multiple runs with the same hyperparameters, we predict the median value.

(b) The relative residual error of all runs, grouped by  $\gamma$  and sorted by  $\alpha$ . Data points slightly perturbed horizontally to aid in visualisation. Points are coloured by relative error.

Figure 7: Comparison of 2D regression and phase regression error.

- The model during SGLD sampling spends a significant portion of the time with better performance than at  $w^*$ . This would correspond to the SGLD sampler training the model. This happens if the localization is small,  $n\beta$  is high and the learning rate is small.
- The model during SGLD sampling spends most of the time with regret comparable to that of a generic policy. This pitfall is not present to the same extent in supervised learning since the cross-entropy loss function is unbounded above and gives non-trivial information even in regions of parameter space in which the loss is high. This pitfall happens when the localization is small,  $n\beta$  is small and the learning rate is high.
- The model during SGLD sampling stabilizes in a region with loss near  $G(w^*)$ , so  $G(w) - G(w^*)$  is small and dominated by noise. This happens when the localization is large and  $n\beta$  is small.

Since the variance of the mean chain regret is larger in the reinforcement learning setting than in supervised learning we use 5 chains instead of the standard 4 in supervised learning.

## C Predicting transitions

In the context of Section 3.4.2 we try to predict transitions based on the hyperparameters  $\alpha, \gamma$ .

Now, all the values of  $\gamma \in \{0.9, 0.95, 0.975, 0.99\}$  are relatively close, but using the value of  $\gamma$  directly as a feature doesn't reflect the hyperbolic nature of the discount factor, as  $\gamma \rightarrow 1$ , the agent becomes "infinitely" far-sighted. So, we instead compute the *effective horizon*  $h = \frac{1}{1-\gamma}$ , and model the number of gradient steps taken for the transition  $\pi^1 \rightarrow \pi^{2b}$  linearly as

$$c_1 + c_2\alpha + c_3h$$

for learned coefficients  $c_1, c_2, c_3$ . We find the best fit to be  $175.52 + 459.20\alpha + 12.00h$ , with a coefficient of determination of  $R^2 = 0.870$ , and a relative error of at worst  $\pm 30\%$ .

## D Model Architecture

The model follows an IMPALA-style convolutional encoder with residual blocks presented in Abdel Sadek et al. (2025), see Figure 8. The previous action is embedded as a one-hot vector of length 4 (with the zero

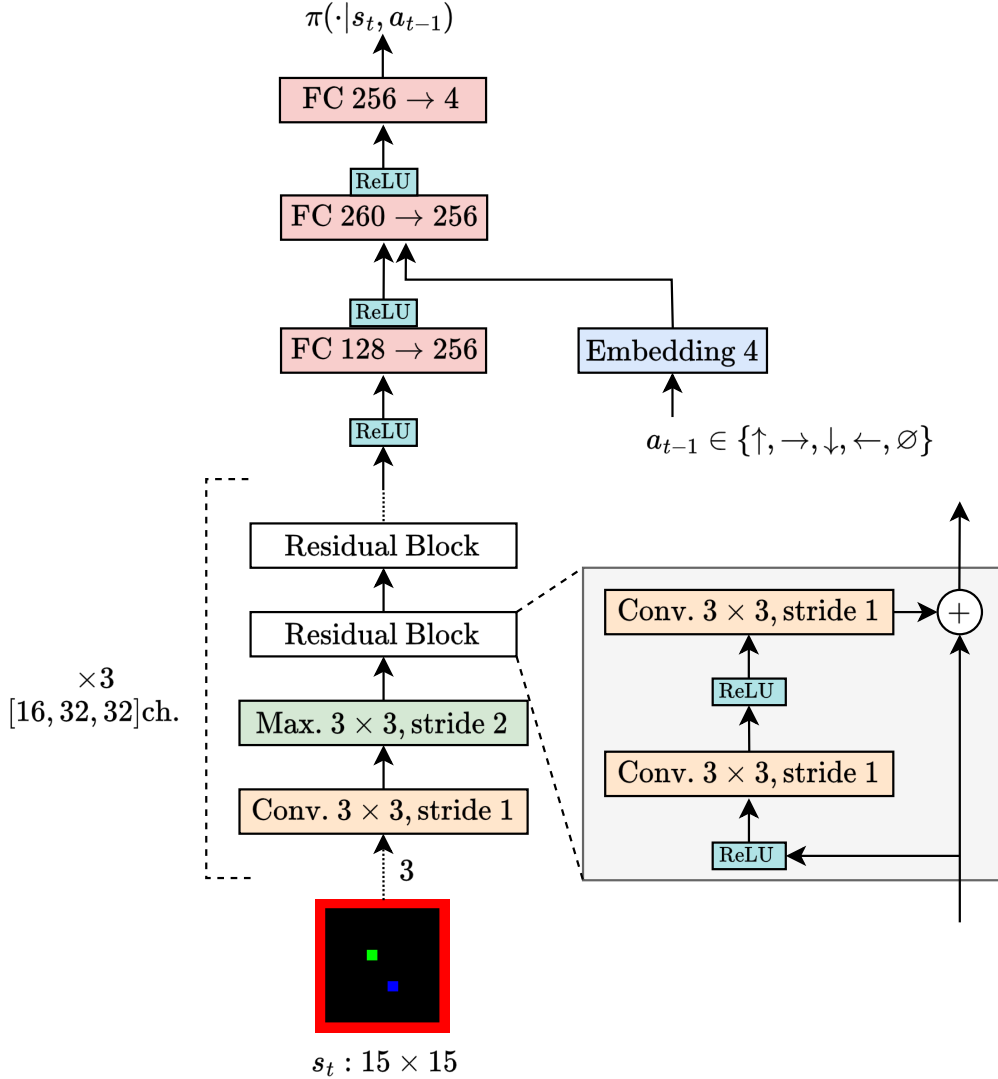


Figure 8: Model architecture diagram. Diagram replicated from Espeholt et al. (2018) with modifications.

vector encoding the lack of a previous action on the first timestep). This then is fed into a small feedforward network (in place of a LSTM) which then feeds into a policy head, from which we obtain the logits over the actions.

The original network in Abdel Sadek et al. (2025) also adds a value head, which has been removed as we make no use of it. At a high level the network maps an input observation  $x \in \mathbb{R}^{C \times H \times W}$  and a previous action  $a_{t-1} \in \{\uparrow, \downarrow, \leftarrow, \rightarrow, \emptyset\}$  to policy logits  $\pi(\cdot|s_t, a_{t-1}) \in \mathbb{R}^4$ , which can be softmaxed to obtain a probability distribution over actions.

## D.1 Convolutional trunk

We let  $\text{Conv}^{c_{\text{in}} \rightarrow c_{\text{out}}}$  denote a  $3 \times 3$  convolution mapping an image with  $c_{\text{in}}$  many input channels to an image with  $c_{\text{out}}$  output channels. The kernel is always  $3 \times 3$ , with a stride of 1, and padding of 1. We let  $\text{MaxPool}$  denote a  $3 \times 3$  max pooling operation with a stride of 2.

The model is then defined as follows.

$$\begin{aligned}
 \text{Model}(s_t, a_{t-1}) &= \text{Encoder}(s_t), \text{Embedding}(a_{t-1}) \rightarrow \text{Linear}(260 \rightarrow 256) \\
 &\rightarrow \text{ReLU} \rightarrow \text{Linear}(256 \rightarrow 4) \\
 \text{Encoder} &= \text{Block}(3, 16) \rightarrow \text{Block}(16, 32) \rightarrow \text{Block}(32, 32) \\
 &\rightarrow \text{ReLU} \rightarrow \text{Flatten} \rightarrow \text{Linear}(128 \rightarrow 256) \rightarrow \text{ReLU} \\
 \text{Block}(c_{\text{in}}, c_{\text{out}}) &= \text{Conv}^{c_{\text{in}} \rightarrow c_{\text{out}}} \rightarrow \text{MaxPool} \rightarrow \text{ResBlock}(c_{\text{out}}) \rightarrow \text{ResBlock}(c_{\text{out}}) \\
 \text{ResBlock}(c)(x) &= x + \text{Conv}^{c \rightarrow c} \left( \text{ReLU}(\text{Conv}^{c \rightarrow c}(\text{ReLU}(x))) \right)
 \end{aligned}$$

## D.2 Previous-action Embedding

The previous action is encoded as a 4-dimensional one-hot vector; the null previous action  $a_0 = \emptyset$  is encoded as the zero vector. This action embedding is concatenated with the observation embedding output from the encoder stack, and then fed into the last feature extractor layer  $\text{Linear}(260 \rightarrow 256)$ .

## D.3 Heads

One linear head reads from the 256-dimensional embedding, and outputs the logits for the actions. Outputs preserve the leading batch/time dimensions of the input, which are not notated for brevity.

## D.4 Hyperparameters

Table 1: Hyperparameters used for all methods and environments.

| Parameter                             | Value                            | Notes/exceptions                                  |
|---------------------------------------|----------------------------------|---|
| <i>Rollouts</i>                       |                                  |   |
| # parallel environments               | 9600                             |   |
| Rollout length                        | 64                               |   |
| # environment steps per gradient step | 614.4k                           | (# parallel environments $\times$ rollout length) |
| Discount factor, $\gamma$             | $\in \{0.9, 0.95, 0.975, 0.99\}$ | Was varied over experiments.                      |
| <i>REINFORCE updates</i>              |                                  |   |
| Number of env steps per run           | 5B                               |   |
| Number of batches per run             | 8138                             | (# [env steps per run/env steps per batch] )      |
| Adam learning rate                    | 5e-5                             |   |
| Learning rate schedule                | constant                         |   |

## D.5 Compute

We perform each training run on a single NVIDIA RTX-4090 24GB GPU. The training process runs at about 450k env steps per second, and each run takes roughly 3 hours. Hyperparameter sweeping for the results used in the paper was roughly 200 runs, at a cost of roughly 600 RTX-4090 hours. LLC estimation was performed on NVIDIA RTX-5090 32GB GPUs, taking roughly 1 hour per sgld chain, meaning 5 GPU hours per checkpoint.

## E Theoretical Foundations of Singular Learning Theory in Reinforcement Learning

### E.1 Markov Problems and the Regret

#### E.1.1 Initial Setup

In this section, by *space* we mean a locally compact Hausdorff space equipped with its Borel  $\sigma$ -algebra. Most of the spaces that we consider will be real analytic manifolds (or more generally real analytic manifolds with corners). If  $M$  is a real analytic manifold we will write  $C^\omega(M)$  for the vector space of real analytic functions on  $M$ . This is a locally convex topological vector space when equipped with the compact-open topology.

Fix a *partially observable Markov decision process* with real analytic manifolds  $\mathcal{S}$  of states,  $\mathcal{A}$  of actions and  $\mathcal{O}$  of observations equipped with volume forms  $ds, da, do$  respectively. Suppose that the expectation value of the reward exists for all state action pairs  $(s, a)$  and denote it by  $r(s, a)$ . Assume that the function  $r$  is real analytic. We fix a natural number  $T_{\max}$  and require that the Markov decision process terminates after  $T_{\max}$  actions.

**Example E.1.** Recall that the Markov decision process is called *finite* if  $\mathcal{S}, \mathcal{A}, \mathcal{O}$  are all finite sets equipped with their counting measures.

**Remark E.2.** In Toussaint and Storkey (2006) Toussaint and Storkey study Markov decision problems of unbounded length by considering an infinite mixture of bounded length decision problems. We will not pursue this approach in the formalization considered below but we expect that the techniques will generalize to their setting.

**Definition E.3.** A *trajectory* is a finite sequence

$$\tau = (s_0, o_0, a_1, s_1, o_1, \dots, a_{T_{\max}}, s_{T_{\max}}, o_{T_{\max}})$$

where  $s_i \in \mathcal{S}, o_i \in \mathcal{O}$  and  $a_i \in \mathcal{A}$ . We write  $\mathcal{T}$  for the real analytic manifold of all trajectories with canonical volume form  $d\tau$ .

If we fix a discount factor  $\gamma \in [0, 1]$ , the *reward of a trajectory* is given by

$$r(\tau) = \sum_{i=1}^{T_{\max}} \gamma^i r(s_{i-1}, a_i).$$

Note that we reuse the symbol  $r$  here. We will no longer need to refer to the reward of a single state-action pair so there will be no ambiguity.

**Definition E.4.** A *policy* is a measurable function  $\pi: \mathcal{O} \rightarrow \Delta(\mathcal{A})$  assigning a probability distribution over actions to each observation. We equip  $\Delta(\mathcal{A})$  with its weak\* topology and write  $\Pi$  for the (non-locally-compact) space of all policies equipped with the compact-open topology.

Policies determine probability distributions on the space  $\mathcal{T}$  of trajectories as follows.

**Definition E.5.** Fix a policy  $\pi \in \Pi$  and an initial distribution  $\Lambda \in \Delta(\mathcal{S})$ . If we write  $p(o_i|s_i)$  and  $p(s_i|a_i)$  for the transition probabilities in the Markov process then we may define a probability measure  $q_\pi d\tau$  on  $\mathcal{T}$  with density function given by

$$q_\pi(\tau) = \Lambda(s_0)p(o_0|s_0) \prod_{i=1}^{T_{\max}} \pi(a_i|o_{i-1})p(s_i|a_i)p(o_i|s_i).$$

**Definition E.6.** A *model* consists of a manifold with corners  $W$  (the *parameter space* of the model) equipped with a volume form  $dw$  and a continuous function  $F: W \rightarrow \Pi$  (the *parameterization*). We will sometimes write  $\pi_w$  for the image  $F(w)$  of a point under the parameterization map and  $q_w$  for the density function  $q_{F(w)}$ .

In order to generalize Watanabe's singular learning theory arguments we will require a *real analyticity* condition on the functions that appear in our optimization problem. Let us clarify what this means.

**Definition E.7.** If  $X, Y$  are real analytic manifolds (possibly with corners), a function  $f: X \rightarrow \Delta(Y)$  is *real analytic* if for all finite subsets  $\{y_1, \dots, y_m\} \subseteq Y$  the function  $\text{proj}_y \circ f: X \rightarrow \Delta^m$  is real analytic, where  $\text{proj}_y$  is the projection onto the  $m$ -simplex spanned by  $\{y_1, \dots, y_m\}$ .

**Assumption E.8.** We say our Markov decision problem and its model are *real analytic* if the reward function  $r$ , the transition functions of the Markov problem and the parameterization map  $F$  are all real analytic. From now on all Markov decision problems are assumed to be real analytic.

**Example E.9.** Finite Markov decision problems are automatically real analytic, and if we parameterize such a problem by a neural network with real analytic activation function (for instance linear or polynomial activations, sigmoids, or the GeLU or swish functions) then the model is also real analytic.

We may now introduce the optimization objective in our reinforcement learning problem, the *regret* function.

**Definition E.10.** The *expected reward* at parameter  $w \in W$  is

$$R(w) = \mathbb{E}_{\tau \sim q_w}(r(\tau)).$$

Suppose that  $R: W \rightarrow \mathbb{R}$  is bounded above and let  $R_{\max} = \sup_{w \in W} R(w)$ . The *regret* at parameter  $w \in W$  is

$$\begin{aligned} G(w) &= R_{\max} - R(w) \\ &= \mathbb{E}_{\tau \sim q_w}(g(\tau)) \end{aligned}$$

where  $g(\tau) = R_{\max} - r(\tau)$ .

**Remark E.11.** If we take  $W$  to be compact then  $R$  is automatically bounded and attains its bounds since it is continuous. Therefore  $G$  is bounded below by zero and attains this lower bound along some non-empty subspace  $W_0 \subseteq W$ .

### E.1.2 Importance Weighting Estimators

For  $n \in \mathbb{N}$  let  $w_1, \dots, w_n$  be a sequence of points in  $W$ . Let  $\tau_1, \dots, \tau_n$  be a sequence of random variables in  $\mathcal{T}$  where  $\tau_i$  is sampled from the distribution  $q_{w_i}$ ; in particular suppose that  $q_{w_i}(\tau_i) > 0$  for all  $i = 1, \dots, n$ . We will define a statistic valued in continuous functions on  $W$  that estimates the regret.

**Definition E.12.** Define a random variable, the *importance sampling regret estimator*, as follows.

$$\begin{aligned} G_n(w) &= \frac{1}{n} \sum_{i=1}^n \frac{q_w(\tau_i)}{q_{w_i}(\tau_i)} g(\tau_i) \\ &= \frac{1}{n} \sum_{i=1}^n \prod_{j=1}^{T_{\max}} \frac{\pi_w(a_{j,i} | o_{j-1,i})}{\pi_{w_i}(a_{j,i} | o_{j-1,i})} g(\tau_i) \end{aligned}$$

where  $a_{j,i}$  represents action  $j$  in trajectory  $\tau_i$  and similarly for the observation  $o_{j-1,i}$ .

Observe that Assumption E.8 guarantees that the random variables  $G_n(w)$  are real analytic function valued. That is,  $G_n$  is real analytic as a function

$$W \times W^n \times \mathcal{T}^n \rightarrow \mathbb{R}$$

defined away from the subspace on which  $q_{w_i}(\tau_i) = 0$ , with poles as this subspace is approached.

We will want to refer to the importance weighted regret of a trajectory frequently enough in the subsequent section that it is worth establishing consistent notation for it.

**Definition E.13.** For  $w, w' \in W$  and  $\tau \in \mathcal{T}$  such that  $q_{w'}(\tau) > 0$  we define

$$f(w, w', \tau) = \frac{q_w(\tau)}{q_{w'}(\tau)} g(\tau).$$

## E.2 Singular Learning Theory for Generalized Bayesian Inference

We will introduce at this point an additional assumption.

**Assumption E.14.** Assume that the parameter space  $W$  is compact.

In particular the set  $W_0 = G^{-1}(0)$  of global minima of the regret is non-empty. Recall that  $W$  is a manifold with corners; we use  $\mathring{W}$  to denote its interior.

### E.2.1 Setup for Generalized Bayesian Inference

In this section we will describe a general setting for generalized Bayesian inference that allows us to study singular learning theory for supervised learning and reinforcement learning, among other situations, in a unified fashion. We will see shortly in Example E.20 that the Markov decision problem setting introduced in the previous section is an example of the situation we will describe now. Our basic setting will comprise the following.

- Let  $X$  be a real analytic manifold equipped with a volume form  $dx$ .
- Let  $w \mapsto q_w dx$  be a real analytic family of signed measures on  $X$  parameterized by  $w \in W$ . Assume that if  $w \in \overset{\circ}{W}$  then  $q_w(x) \neq 0$  for all  $x \in X$ .
- Let  $g: X \rightarrow \mathbb{R}$  and  $h: X \rightarrow \mathbb{R}_{\geq 0}$  be real analytic functions.

**Definition E.15.** The *loss function*  $G: W \rightarrow \mathbb{R}$  is defined to be:

$$G(w) = \int (g(x)q_w(x) - h(x))dx.$$

**Assumption E.16.** Suppose that  $\min(G(w)) = 0$ . We will assume that if  $w \in W$  is a parameter so that  $G(w) = 0$  (an *optimal parameter*) then the set

$$\{x: g(x)q_w(x) - h(x) \neq 0\}$$

has Lebesgue measure zero.

**Remark E.17.** If we're interested in optimization for  $G(w)$  observe that the choice of  $h$  only changes  $G$  by an additive constant, so one can try to choose  $h$  in such a way that the assumption is satisfied.

**Definition E.18.** Given a sequence of points  $w_1, \dots, w_n$  in  $\overset{\circ}{W}$  and samples  $x_i \sim q_{w_i}$  for  $i = 1, \dots, n$ , define a random variable, the *importance sampling estimator*, by

$$G_n(w) = \frac{1}{n} \sum_{i=1}^n f(w, w_i, x_i) \quad (18)$$

where  $f(w, w_i, x_i) = \frac{q_w(x_i)}{q_{w_i}(x_i)} g(x_i) - \frac{1}{q_{w_i}(x_i)} h(x_i)$ .

**Example E.19.** Our first example is considered in Watanabe's original work Watanabe (2009): supervised learning for a model where the true distribution is realizable. Choose any compact parameter space  $W$  and sample space  $X$  and specify a real analytic family  $p_w$  of probability distributions on  $X$ .

Let  $q_w(x) = -\log p_w(x)$ . Fix a point  $w^* \in W$  and let  $g(x) = p_{w^*}(x)$  and  $h(x) = p_{w^*}(x) \log p_{w^*}(x)$ . Then

$$G(w) = \int p_{w^*}(x) \log \frac{p_{w^*}(x)}{p_w(x)} dx = \text{KL}(p_{w^*} \parallel p_w),$$

that is, the loss agrees with the Kullback–Leibler divergence from the “true distribution”  $p_{w^*}$ . A point  $w$  is optimal if  $p_w = p_{w^*}$ . If so then  $g(x)q_w(x) - h(x) = 0$  for all  $x$ , so Assumption E.16 holds automatically.

For the estimators in this example we generalize Definition E.18 slightly in this case and instead consider  $x_i$  samples from  $p_{w^*}$  for  $i = 1, \dots, n$  with

$$f(w, w^*, x_i) = \frac{q_w(x_i)}{p_{w^*}(x_i)} g(x_i) - \frac{1}{p_{w^*}(x_i)} h(x_i).$$

so that

$$G_n(w) = \frac{1}{n} \sum_{i=1}^n g(x_i) f(w, w^*, x_i) = -\frac{1}{n} \sum_{i=1}^n \log \frac{p_w(x_i)}{p_{w^*}(x_i)}.$$

The proof of the main results continues to hold for this modified definition of  $f$  but we do not track this modification carefully in the text below; in this case our results coincide with those in Watanabe's original work.

**Example E.20.** Now let us consider a Markov decision problem as in E.1 and let  $X = \mathcal{T}$  be the space of trajectories. Let  $\Pi$  be the space of policies, and choose an analytic parameterization map  $F: W \rightarrow \Pi$  sending  $w$  to  $\pi_w$ . Let  $q_w$  be the distribution on  $\mathcal{T}$  associated to this choice of policy. If  $\tau \in \mathcal{T}$ , let  $g(\tau)$  be defined as in Definition E.10 and let  $h(\tau) = 0$ .

Assumption E.16 is not necessarily satisfied; it holds if optimal policies pursue optimal trajectories with probability one. We will discuss this further in Section E.2.4 below.

Note that in the Markov decision problem setting Assumption E.16 holds in particular if the decision problem has deterministic transition functions, meaning that the distributions  $p(o|s)$  and  $p(s|a)$  are all delta distributions. Say a trajectory  $\tau$  is *reachable* for an MDP if there exists  $w \in W$  so that  $q(w, \tau) > 0$ .

**Proposition E.21.** Let  $\pi_w$  be an optimal policy in a Markov decision problem. If the problem has deterministic transition functions then  $g(\tau) \geq 0$  for all reachable trajectories  $\tau \in \mathcal{T}$  and  $q_w(\tau) = 0$  if and only if  $g(\tau) > 0$ . In particular Assumption E.16 holds.

*Proof.* If the deterministic transition condition holds then for all policies  $\pi_w$  either  $q_w(\tau) = 0$  or

$$q_w(\tau) = \Lambda(s_1) \prod_{i=1}^{N-1} \pi_w(a_i | s_i)$$

where  $\Lambda$  denote the distribution on initial states. In particular

$$G(w) = \sum_{\tau: q_w(\tau) \neq 0} \Lambda(s_0) \left( \prod_{i=1}^{N-1} \pi_w(a_i | o_{i-1}) \right) g(\tau).$$

If  $\tau$  is a reachable trajectory we may, using the deterministic transition condition, choose a deterministic policy  $w_0$  so that  $q(w_0, \tau) = 1$ . In particular  $G(w) = q_w(\tau)g(\tau)$ , which implies  $g(\tau) \geq 0$  with equality if and only if  $w$  is optimal. On the other hand, if  $w$  is an optimal policy then  $G(w) = 0$ , so the fact that  $g(\tau) \geq 0$  for all summands implies  $q_w(\tau) = 0$  if  $g(\tau) > 0$ .  $\square$

Given the above setup, we will study *generalized Bayesian inference* in the sense of Zhang (2006); Bissiri et al. (2016) for the loss function  $G$ . To that end, fix an analytic prior probability distribution  $\phi(w)dw$  on  $W$  and a real number  $\beta > 0$ .

**Definition E.22.** The *generalized tempered posterior* or *Gibbs posterior* associated to  $\phi, \beta$  and the random variable  $G_n$  is the probability distribution

$$\mu_n^\beta(U) \propto \int_U \exp(-n\beta G_n(w)) \phi(w) dw.$$

**Remark E.23.** The generalized posterior with  $\beta = 1$  is determined canonically by Theorem 1 of Bissiri, Holmes and Walker Bissiri et al. (2016). Indeed, given a prior distribution  $\phi(w)dw$  and the loss function  $f(w, w', x)$  we consider the collection of all probability measures of the form

$$\mu_{(\psi)} \propto \psi(f(w, w', x), \phi(w)) dw,$$

where  $\psi$  is a continuous function of two real variables. Bissiri, Holmes and Walker's argument shows that the generalized posterior is uniquely characterized within this family by the condition that

$$\psi(f(w, w', x_2), \psi(f(w, w', x_2), \phi(w))) = \psi(f(w, w', x_1) + f(w, w', x_2), \phi(w)).$$

Their proof applies in the case where  $W$  is countable and discrete, but we note that since the function  $\psi(f(w, w', x_2), \psi(f(w, w', x_2), \phi(w))) - \psi(f(w, w', x_1) + f(w, w', x_2), \phi(w))$  is continuous in  $w \in W$  it is enough to show that it vanishes on a countable dense subset of  $W$ . Together with Remark E.26 below we see that the generalized tempered posterior is canonically characterized by the loss function under natural assumptions.

Our goal is to prove theorems about the properties of this posterior distribution, generalizing the arguments of Watanabe. Our main results are as follows.

**Theorem E.24.** 1. *Standard form of the estimator:* If  $w_0 \in W$  is an optimal parameter then we may find a log resolution  $\varpi$  of  $G$  locally near  $w_0$  and a local coordinate  $u$  for which

$$G_n(\varpi(u)) = u^{2k} - n^{-1/2}u^k\xi_n(u)$$

where  $\xi_n(u)$  converges in distribution to a standard Gaussian.

2. *Asymptotics of the posterior:* Let  $U \subseteq W$  be an open set. The generalized tempered posterior has asymptotic behavior

$$\int_U \exp(-n\beta G_n(w))\phi(w)dw \sim n^{-\lambda} \log n^{m+1}$$

where  $\lambda, m$  are the log canonical threshold and multiplicity of  $G$  on the set  $U$ .

3. *Expectation of the total loss:* Let  $w_0$  be a local minimum of  $G$ . Let  $\mathbb{E}_n^\beta$  represent the expected value with respect to the tempered posterior  $\mu_n^\beta$ . Let  $\beta$  be a positive function on the natural numbers such that  $\beta(n)$  converges as  $n \rightarrow \infty$ . Then there exists an open neighborhood  $U'$  of  $w_0$  so that for all subneighborhoods  $U \subseteq U'$

$$\mathbb{E}_n^\beta(nG_n(w)|_U) = nG_n(w_0) + \frac{\lambda}{\beta} + o_P(\log n).$$

## E.2.2 Convergence of Error Terms

As the first step in our proof of Theorem E.24 we will need to establish a version of the results from (Watanabe, 2009, Section 5) that applies in the generalized Bayesian inference setting in which our samples  $x_i$  are not identically distributed. We will first establish that a version of the central limit theorem may be applied to our importance weighted regret estimators.

**Lemma E.25.** The expectation value of the importance weighted loss estimator is  $\mathbb{E}(G_n(w)) = G(w)$  for all  $n$ .

*Proof.* This is a straightforward computation:

$$\begin{aligned} \mathbb{E}(G_n(w)) &= \frac{1}{n} \sum_{i=1}^n \mathbb{E}_{x_i \sim q_{w_i}} \left( \frac{q_w(x_i)}{q_{w_i}(x_i)} g(x_i) - \frac{1}{q_{w_i}(x_i)} h(x_i) \right) \\ &= \frac{1}{n} \sum_{i=1}^n \left( \int (g(x_i)q_w(x_i) - h(x_i))dx_i \right) \\ &= G(w). \end{aligned}$$

□

**Remark E.26.** This property, together with the *additivity* condition in the statistics  $G_n$  given by equation 18 naturally characterizes the importance weighted loss estimator. Indeed, consider the case  $n = 1$  (where we usually denote  $G_1$  by  $f$ ). The condition  $\mathbb{E}(f(w, w')) = G(w)$  may be rewritten as

$$\int \left( g(x) \frac{q_w(x)}{q_{w'}(x)} - h(x) \frac{1}{q_{w'}(x)} \right) - f(w, w', x)dx = 0.$$

So our definition of the importance weighted estimator  $f(w, w')$  is the unique function for which the integrand identically vanishes.

For the rest of this section we will impose some conditions on our importance weighting estimator. Suppose  $w, w_i \in \mathring{W} \setminus W_0$  and  $w_i \rightarrow w^*$  as  $i \rightarrow \infty$  for some  $w^* \in \mathring{W} \setminus W_0$ . Suppose that the importance weighted regret  $f(w, w', x)$  has finite positive variance  $0 < \sigma(w, w') < \infty$  for all  $w' \in \mathring{W} \setminus W_0$ . Suppose also that there exists  $\delta > 0$  so that the  $2 + \delta$ -moment of  $f(w, w', x)$  exists for all  $w' \in \mathring{W} \setminus W_0$ .

**Proposition E.27.** The random variables

$$\psi_n(w) = \frac{\sqrt{n}(G(w) - G_n(w))}{\sigma(w, w^*)}$$

converge in distribution to  $N(0, 1)$  as  $n \rightarrow \infty$ .

*Proof.* We have just seen in Lemma E.25 all individually have expected value  $G(w)$ . To establish the result we will verify Lyapounov's condition, that is, we need to check that, for some  $\delta > 0$ ,

$$\frac{\sum_{i=1}^n \|f(w, w_i, x_i) - G(w)\|_{2+\delta}^{2+\delta}}{(\sum_{i=1}^n \|f(w, w_i, x_i) - G(w)\|_2^2)^{\frac{2+\delta}{2}}} \rightarrow 0$$

as  $n \rightarrow \infty$ . Choose  $\delta > 0$  so that the relevant moment exists. Then since  $w_i \rightarrow w^*$  we may find a compact subspace of  $\mathring{W} \setminus W_0$  containing  $w^*$  and  $w_i$  for all  $i$ , and therefore may find we may choose constants  $c_2, c_{2+\delta} > 0$  so that

$$\|f(w, w_i, x) - G(w)\|_2 \geq c_2, \quad \|f(w, w_i, x) - G(w)\|_{2+\delta} \leq c_{2+\delta}$$

for all  $i \geq 1$ . Then

$$\begin{aligned} \frac{\sum_{i=1}^n \|f(w, w_i, x_i) - G(w)\|_{2+\delta}^{2+\delta}}{(\sum_{i=1}^n \|f(w, w_i, x_i) - G(w)\|_2^2)^{\frac{2+\delta}{2}}} &\leq \frac{n c_{2+\delta}^{2+\delta}}{n^{\frac{2+\delta}{2}} c_2^2} \\ &= \frac{c_{2+\delta}^{2+\delta}}{c_2^2} n^{-\frac{\delta}{2}} \\ &\rightarrow 0 \end{aligned}$$

as  $n \rightarrow \infty$ . Lyapounov's central limit theorem then says that

$$\frac{1}{n} \sum_{i=1}^n \frac{G(w) - f(w, w_i, x_i)}{\sigma(w, w_i)} \rightarrow N(0, 1)$$

in distribution as  $n \rightarrow \infty$ .

To complete the proof, observe that  $w_i \rightarrow w^*$  implies that  $\frac{1}{\sigma(w, w_i)} \rightarrow \frac{1}{\sigma(w, w^*)}$  as  $i \rightarrow \infty$  since  $\frac{1}{\sigma(w, -)}$  is continuous as a function on  $\mathring{W} \setminus W_0$ . As before we choose a compact subset  $V \subseteq \mathring{W} \setminus W_0$  containing the sequence  $w_i$  and the point  $w^*$ , and find a positive constant  $A$  so that  $|G(w) - f(w, w', x)| \leq A$  for all  $x \in X, w' \in V$ . Then

$$\begin{aligned} \left| \frac{1}{n} \sum_{i=1}^n \frac{G(w) - f(w, w_i, x_i)}{\sigma(w, w_i)} - \frac{1}{n} \sum_{i=1}^n \frac{G(w) - f(w, w_i, x_i)}{\sigma(w, w^*)} \right| &\leq \frac{1}{n} \sum_{i=1}^n \left| (G(w) - f(w, w_i, x_i)) \left( \frac{1}{\sigma(w, w_i)} - \frac{1}{\sigma(w, w^*)} \right) \right| \\ &\leq \frac{A}{n} \sum_{i=1}^n \left| \frac{1}{\sigma(w, w_i)} - \frac{1}{\sigma(w, w^*)} \right| \\ &\rightarrow 0 \end{aligned}$$

as  $n \rightarrow \infty$ . □

We will use this version of the central limit theorem to establish uniform convergence properties of the random variables  $\psi_n(w)$  over compact subsets of  $\mathring{W} \setminus W_0$ . Our goal is an analogue of (Watanabe, 2009, Theorem 5.9). More specifically we will prove the following.

**Theorem E.28.** Let  $K \subseteq \mathring{W} \setminus W_0$  be a compact subset. The sequence  $\psi_n|_K$  of  $C^\omega(K)$ -valued random variables converges in distribution in  $C^\omega(K)$  to a random variable  $\psi|_K$ .

Our proof strategy – following Watanabe – will combine Prokhorov's theorem, telling us that is we can prove  $\psi_n|_K$  is a uniformly tight sequence then it admits a convergent subsequence, with Proposition E.27 telling us that the sequence  $\psi_n(w)$  converges pointwise for  $w \in \mathring{W} \setminus W_0$ . We will begin with a sequence of lemmas that will together prove uniform tightness. Throughout these lemmas we fix a compact subset  $K \subseteq \mathring{W} \setminus W_0$ .

**Lemma E.29.** Let  $s > 2$  be an even integer. Suppose that  $f(w, w', -)$  is a random variable of class  $L^s(q_w)$  for all  $w, w' \in W$ . Then  $\psi_n(w)$  is also of class  $L^s(q_w)$  for all  $w \in W$ .

*Proof.* If  $n = 1$  we have  $\psi_1(w)(x) = \frac{1}{\sigma(w, w^*)}(\mathbb{E}(f(w, w', x)) - f(w, w', x))$ . Since  $q_w$  is a probability measure and  $f(w, w', -)$  is of class  $L^s(q_w)$  so is  $\psi_1(w)$ . For  $n > 1$ ,  $\psi_n(w)$  is a linear combination of  $\psi_1(w)$  random variables and therefore is also of class  $L^s(p_w)$ .  $\square$

**Lemma E.30.** Let  $s > 2$  be an even integer. Suppose that  $\psi_n(w)$  is a random variable of class  $L^s(q_w)$  for all  $w \in W$ . Then

$$\limsup_{n \rightarrow \infty} \left\| \sup_{w \in K} \psi_n(w) \right\|_s < \infty.$$

*Proof.* We will generalize the argument given by in (Watanabe, 2009, Theorem 5.7, 5.8). Recall that

$$\begin{aligned} \psi_n(w) &= \frac{1}{\sqrt{n}} \sum_{i=1}^n \frac{G(w) - f(w, w_i, x_i)}{\sigma(w, w^*)} \\ &= \frac{1}{\sqrt{n}} \sum_{i=1}^n \tilde{f}(w, w_i, x) \end{aligned}$$

where

$$\tilde{f}(w, w_i, x) = \frac{G(w) - f(w, w_i, x)}{\sigma(w, w^*)}.$$

The random variable  $\tilde{f}$  is real analytic as a function of  $W \times W$ . Since  $w_i \rightarrow w^*$  we may assume without loss of generality that all  $w_i$  lie inside a polydisk  $D \subseteq W$  of absolute convergence around  $w^*$  in the second variable. Indeed,

$$\begin{aligned} \left\| \sup_{w \in K} \psi_n(w) \right\|_s &= \left\| \frac{1}{\sqrt{n}} \sum_{i=1}^n \sup_{w \in K} \tilde{f}(w, w_i, x) \right\|_s \\ &\leq \left\| \frac{1}{\sqrt{n}} \sum_{i=1}^{m-1} \sup_{w \in K} \tilde{f}(w, w_i, x) \right\|_s + \left\| \frac{1}{\sqrt{n}} \sum_{i=m}^n \sup_{w \in K} \tilde{f}(w, w_i, x) \right\|_s \\ \implies \lim_{n \rightarrow \infty} \left\| \sup_{w \in K} \psi_n(w) \right\|_s &\leq \lim_{n \rightarrow \infty} \left\| \frac{1}{\sqrt{n}} \sum_{i=m}^n \sup_{w \in K} \tilde{f}(w, w_i, x) \right\|_s \end{aligned}$$

for all  $m \geq 1$ .

Therefore we may choose a finite set of polydisks covering  $K$  with centers  $\{z\}$  so that we can expand  $\psi_n$  as an absolutely convergent series

$$\psi_n(w) = \frac{1}{\sqrt{n}} \sum_{i=1}^n \sum_{\alpha \in \mathbb{Z}^d} \sum_{\alpha' \in \mathbb{Z}^d} a_{\alpha, \alpha'}(x_i) (w - z)^\alpha (w_i - w^*)^{\alpha'}$$

where  $a_{\alpha, \alpha'}(x)$  is of class  $L^s$ . It is sufficient to establish the bound on  $\mathbb{E}(\sup_{w \in K} |\psi_n(w)|^s)$  for each of these finitely many polydisks. On such a polydisk we have

$$\begin{aligned} \left\| \sup_{w \in K} \psi_n(w) \right\|_s &= \left\| \sup_{w \in K} \sum_{\alpha \in \mathbb{Z}^d} \sum_{\alpha' \in \mathbb{Z}^d} (w - z)^\alpha (w_i - w^*)^{\alpha'} \left( \frac{1}{\sqrt{n}} \sum_{i=1}^n a_{\alpha, \alpha'}(x_i) \right) \right\|_s \\ &\leq \left\| \sum_{\alpha \in \mathbb{Z}^d} \sum_{\alpha' \in \mathbb{Z}^d} R^\alpha R'^{\alpha'} \left( \frac{1}{\sqrt{n}} \sum_{i=1}^n a_{\alpha, \alpha'}(x_i) \right) \right\|_s \\ &\leq \sum_{\alpha \in \mathbb{Z}^d} \sum_{\alpha' \in \mathbb{Z}^d} R^\alpha R'^{\alpha'} \left( \left\| \frac{1}{\sqrt{n}} \sum_{i=1}^n a_{\alpha, \alpha'}(x_i) \right\|_s \right) \end{aligned}$$

where  $R$  and  $R'$  are elements of  $\mathbb{R}_{>0}^d$  and  $R^\alpha = \prod_{j=1}^d R_j^{\alpha_j}$ . We need to verify that this series is uniformly bounded in  $n$ .

We will do this by showing

$$\left\| \frac{1}{\sqrt{n}} \sum_{i=1}^n a_{\alpha, \alpha'}(x_i) \right\|_s \leq s \|a_{\alpha, \alpha'}\|_{s, w^*}.$$

where by  $\|\cdot\|_{s, w^*}$  we mean the  $L^s$  norm with respect to the distribution  $p_{w^*}$ . Since  $s \geq 1$  and the power series expansion for  $\psi_n(w)$  is absolutely convergent on the given domain the  $\alpha, \alpha'$  sum still converges and we obtain the desired uniform bound.

Let us consider any analytic function  $a: \mathbb{R} \rightarrow \mathbb{R}$  and consider the argument in (Watanabe, 2009, Theorem 5.7). Without the assumption that the random variables  $X_i$  are identically distributed Watanabe's argument still establishes

$$\begin{aligned} \left\| \frac{1}{\sqrt{n}} \sum_{i=1}^n a(x_i) \right\|_s^s &= n^{-s/2} \mathbb{E} \left( \sum_{j \neq 1} \binom{s}{j} \left( \sum_{i=1}^{n-1} a(x_i) \right)^{s-j} a(x_n)^j \right) \\ &\leq n^{-s/2} \sum_{j \neq 1} \binom{s}{j} \left\| \sum_{i=1}^{n-1} a(x_i) \right\|_s^{s-j} \|a\|_{s, w_n}^j \\ &= \frac{1}{\sqrt{n}} \left( \left\| \sum_{i=1}^{n-1} a(x_i) \right\|_s + \|a\|_{s, w_n} \right)^s - s \left\| \sum_{i=1}^{n-1} a(x_i) \right\|_s^{s-1} \|a\|_s. \end{aligned}$$

The argument in *loc. cit.* then establishes that

$$\begin{aligned} y_{n+1} &\leq F_n(y_n) \\ \text{where } y_n &= \mathbb{E} \left( \left( \frac{1}{\|a\|_{s, w_{n+1}} \sqrt{n}} \sum_{i=1}^n f(X_i) \right)^s \right) \\ \text{and } F_n(y) &= \frac{y}{1 + s/2n} \left( 1 + \frac{s(s-1)}{2ny^{2/s}} \left( 1 + \frac{1}{\sqrt{ny^{1/s}}} \right)^{s-2} \right), \end{aligned}$$

a monotonic function of one variable. Finally Watanabe checks that  $F_n((s-1)^s) \leq (s-1)^s$ . If we know that  $y_1 \leq (s-1)^s$  then, by induction, we will have that  $y_n \leq (s-1)^s$  for all  $s$ , and therefore that

$$\left\| \frac{1}{\sqrt{n}} \sum_{i=1}^n a_{\alpha, \alpha'}(x_i) \right\|_s \leq (s-1) \|a\|_{s, w_{n+1}} \leq s \|a\|_{s, w^*},$$

again truncating the sequence  $w_i \rightarrow w^*$  if necessary.

To conclude we check the base case for our induction. We have

$$y_1 = \left( \frac{\|a\|_{s, w_1}}{\|a\|_{s, w_2}} \right)^s.$$

Since  $w_i \rightarrow w^*$  the sequence  $\|a\|_{s, w_i}$  is a Cauchy sequence. By choosing  $m$  sufficiently large and removing the first  $m$  terms from the sequence  $w_i$  we may assume  $y_1 < 1 + \varepsilon$  for any  $\varepsilon > 0$ . In particular  $y_1 < (s-1)^s$  for any  $s > 2$ .  $\square$

**Lemma E.31.** For every  $\varepsilon > 0$  there exists a compact subset  $C_\varepsilon \subseteq C^\omega(K)$  for which

$$\mathbb{P}(\psi_n|_K \in C_\varepsilon) > 1 - \varepsilon.$$

*Proof.* We will prove this in two steps. First choose an even integer  $s > 2$  as Lemma E.30 and use the lemma to find  $C > 0$  so that

$$\mathbb{E} \left( \sup_{w \in K} |\psi_n(w)|^s \right) < C$$

for all  $n$ . Therefore Markov's lemma implies that, for all  $M > 0$ ,

$$\begin{aligned} \mathbb{P}(\sup_{w \in K} |\psi_n(w)| \geq M) &< \frac{C}{M^s} \\ \implies \mathbb{P}(\sup_{w \in K} |\psi_n(w)| < M) &\geq 1 - \frac{C}{M^s} \end{aligned}$$

We therefore define  $C'_\varepsilon$  to be the set

$$C'_\varepsilon = \{\psi \in C^\omega(K) : \sup_{w \in K} |\psi(w)| < \left(\frac{C}{\varepsilon}\right)^{1/s}\},$$

a closed ball in the  $L^\infty$  topology on  $C^\omega(K)$ . Now, these closed balls are not compact, so we will need to find a compact subspace  $C_\varepsilon \subseteq C'_{\varepsilon/2}$  of measure  $> 1 - \varepsilon$ . Since  $C'_{\varepsilon/2}$  is already uniformly bounded, by the Arzelà–Ascoli theorem it suffices to find an equicontinuous subspace of measure  $> 1 - \varepsilon$ .

Choose a Riemannian metric on  $W$  and let

$$D_{k,\delta} = \{\psi \in C^\omega(K) : \sup_{\|w-w'\| < \delta} |\psi(w) - \psi(w')| < \frac{1}{k}\}.$$

We will find a sequence of values  $\delta_k$  so that

$$\mathbb{P}(\psi_n \in D_{k,\delta_k}) \geq 1 - 2^{-k-1}\varepsilon,$$

so that  $C_\varepsilon = C'_{\varepsilon/2} \cap \bigcap_{k=1}^{\infty} D_{k,\delta_k}$  is a compact subset of measure greater than  $1 - \varepsilon$ .

So, to conclude, we check

$$\begin{aligned} \mathbb{P}(\sup_{\|w-w'\| < \delta} |\psi_n(w) - \psi_n(w')| \geq \frac{1}{k}) &= P(\sup_{\|w-w'\| < \delta} |\psi_n(w) - \psi_n(w')|^s \geq \frac{1}{k^s}) \\ &\leq k^s \mathbb{E}(\sup_{\|w-w'\| < \delta} |\psi_n(w) - \psi_n(w')|^s) \\ &\leq k^s \delta^s \mathbb{E}(\sup_{w \in K} \|\nabla \psi_n(w)\|^s) \end{aligned}$$

by the mean value theorem. Since  $\psi_n(w) \in L^s$  so is  $\nabla \psi_n$ , so the expectation value on the last line above is finite, and therefore

$$\mathbb{P}(\sup_{\|w-w'\| < \delta} |\psi_n(w) - \psi_n(w')| \geq \frac{1}{k}) \rightarrow 0$$

as  $\delta \rightarrow 0$ , which implies the desired claim.  $\square$

**Remark E.32.** The argument given for this claim in (Watanabe, 2009, Example 5.3) requires an additional step since closed balls in the  $L^\infty$  topology on infinite spaces are not compact. This point and the correction used above were communicated to us by Rohan Hitchcock.

**Corollary E.33.** The sequence  $\psi_n|_K$  of  $C^\omega(K)$ -valued random variables is uniformly tight.

We may now prove the main result of this section.

*Proof of Theorem E.28.* Applying Prokhorov's theorem, Corollary E.33 tells us that  $\psi_n(w)$  has a convergent subsequence. Now Proposition E.27 says that  $\psi_n(w)$  converges in distribution pointwise for  $w \in K$ , and therefore  $\psi_n(w)$  converges in  $C^\omega(K)$  to a random variable  $\psi|_K$ .  $\square$

### E.2.3 Resolution of Singularities

Our next goal is to establish part (1) of Theorem E.24. That is, we will give a local (in parameter space) description of the importance weighted estimator  $G_n$  and the empirical process  $\psi_n$  in a standard form that is comparatively easy to manipulate. We will do this by fixing a *log resolution* of the zero set  $W_0 \subseteq W$  of the loss function. We recall the fundamental construction as originally developed by Hironaka (1964).

**Definition E.34.** A local *log resolution* of  $G$  at a point  $w^* \in W_0 \subseteq W$  is a proper real analytic map  $\varpi: \mathcal{M} \rightarrow W$  of real analytic manifolds with corners such that

1.  $\varpi$  restricts to an isomorphism on  $\varpi^{-1}(\mathring{W} \setminus W_0)$ .
2. We can choose a chart  $U$  for  $\mathcal{M}$  centered around any point in  $\varpi^{-1}(w^*)$  with coordinate  $u$  in which

$$\det \text{Jac}(\varpi)(u) = b(u) u_1^{h_1} \cdots u_d^{h_d}$$

for an invertible analytic function  $b$  and

$$G(\varpi(u)) = \begin{cases} \pm u_1^{2k_1} \cdots u_d^{2k_d} & \text{if } w^* \in \mathring{W} \\ \pm u_1^\ell u_2^{2k_2} \cdots u_d^{2k_d} & \text{if } w^* \in \partial W \end{cases}$$

where in the latter case  $U$  is isomorphic to a half-space in  $\mathbb{R}^d$  and  $u_1$  is a normal coordinate to the boundary. The constants  $h_i$ ,  $k_i$  and  $\ell$  are non-negative integers.

Choose a point  $w^* \in W_0$ , a local log resolution  $\varpi$  and a chart  $U$  around this minimum. Let  $U_0 = \varpi^{-1}(W_0) \cap U$  and let  $K$  be a compact subset of  $\mathring{U} \setminus U_0$ . In this chart our importance weighted loss may be usefully expressed in a standard way – in normal crossings form – parallelling (Watanabe, 2009, Main Theorem 1). We will begin by representing the random variable  $f$  from Definition E.18 in normal crossings form.

**Proposition E.35.** There exists real analytic functions  $a, b$  on  $X \times U \times W$  so that we may locally expand

$$f(\varpi(u), w', x) = a(u, w', x) u_1^{\ell/2} u_2^{k_2} \cdots u_d^{k_d} + b(u, w', x),$$

so that for all  $w' \in W$

$$\begin{aligned} \int_X a(u, w', x) q_{w'}(x) dx &= u_1^{\ell/2} u_2^{k_2} \cdots u_d^{k_d} \\ \int_X b(u, w', x) q_{w'}(x) dx &= 0, \end{aligned}$$

and where all Taylor coefficients of  $b$  of order  $\geq (\ell/2, k_2, \dots, k_d)$  vanish identically.

*Proof.* We obtain  $a, b$  by forming the Taylor expansion in  $u$  of the analytic function  $f(\varpi(u), w', x)$  and splitting the resulting sum into the sum of those Taylor terms of order at least  $u_1^{\lceil \ell/2 \rceil} u_2^{k_2} \cdots u_d^{k_d}$ , and the sum of those Taylor terms of smaller degree in at least one variable. Having done so, by Lemma E.25 and the definition of the log resolution we have

$$\begin{aligned} \int_X (a(u, w', x) u_1^{\ell/2} u_2^{k_2} \cdots u_d^{k_d} + b(u, w', x)) q_{w'}(x) dx &= \mathbb{E}(f(u, w', x)) \\ &= G(\varpi(u)) \\ &= \pm u_1^\ell \cdots u_d^{2k_d}. \end{aligned}$$

We obtain the desired expressions by comparing the orders of Taylor coefficients on the two sides and replacing  $a$  by  $-a$  if  $G(\varpi(u)) = -u_1^\ell \cdots u_d^{2k_d}$ .  $\square$

**Theorem E.36.** In the local chart  $U$  we may express the importance weighted loss as

$$G_n(\varpi(u)) = u^{2k} - u^k \xi_n(u) - \omega_n(u)$$

where  $u^{2k} = u_1^\ell u_2^{2k_2} \cdots u_d^{2k_d}$  and  $u^k = u_1^{\ell/2} u_2^{k_2} \cdots u_d^{k_d}$ . The random variables

$$\xi_n(u) + \omega_n(u) u^{-k} = \frac{1}{\sqrt{n}} \left( \sum_{i=1}^n a(u, w_i, x_i) - \mathbb{E}(a(u, w_i, x_i)) \right) + \frac{1}{\sqrt{n}} \left( \sum_{i=1}^n b(u, w_i, x_i) \right) u^{-k}$$

converge to a Gaussian in distribution uniformly in  $K$ .

*Proof.* By Theorem E.28 and Proposition E.27 we know that  $\sqrt{n}(G(w) - G_n(w)) \rightarrow \mathcal{N}(0, \sigma(w, w^*)^2)$  in distribution uniformly over compact subspaces of  $\mathring{W} \setminus W_0$ . In particular for the resolution  $\varpi$  we have

$$\begin{aligned} & \sqrt{n}(G(\varpi(u)) - G_n(\varpi(u))) \rightarrow \mathcal{N}(0, \sigma(w, w^*)^2) \\ \implies & \frac{1}{\sqrt{n}} \sum_{i=1}^n (u^{2k} - a(u, w_i, x_i)u^k + b(u, w_i, x_i)) \rightarrow \mathcal{N}(0, \sigma(\varpi(u), w^*)^2) \\ \Leftrightarrow & -\xi_n(u)u^k + \omega_n(u) \rightarrow \mathcal{N}(0, \sigma(\varpi(u), w^*)^2) \\ \Leftrightarrow & \xi_n(u) + \omega_n(u)u^{-k} \rightarrow \mathcal{N}(0, \sigma(\varpi(u), w^*)^2 u^{-2k}) \end{aligned}$$

in distribution uniformly in  $K$ .  $\square$

In order to proceed from here we will establish situations where the summands  $\omega_n$  converge vanish.

#### E.2.4 Free Energy Asymptotics

Let us now return to Theorem E.24, in this section we will address part (2), concerning the asymptotic behavior of the generalized posterior distribution. In order to establish clear asymptotics we will need to guarantee that the lower order terms in the importance weighted loss estimators – the terms  $\omega_n$  from Theorem E.36 – do not contribute to the posterior. This is not likely to hold in general, we will establish it under the condition that Assumption E.16 holds, i.e. that if  $w^* \in W$  minimizes the loss then the set

$$\{x: g(x)q_{w^*}(x) - h(x) \neq 0\} \subseteq X$$

has Lebesgue measure zero.

Our initial aim is to show the following.

**Proposition E.37.** If  $q_w$  is a probability distribution for all  $w$  and Assumption E.16 holds then  $\omega_n = 0$  for all  $n$ .

**Remark E.38.** Proposition E.37 is very close to the condition of *relatively finite variance* that appears in Watanabe (2018). In the general case where  $q_w$  is merely a signed measure (which includes the density estimation problem originally considered by Watanabe) the relatively finite variance condition is what is needed to establish  $\omega_n = 0$ . This is, however, implied by Assumption E.16 in the positive case. Indeed, recall that the function  $f$  has *relatively finite variance* if

$$\sup_{w \in \mathring{W} \setminus W_0} \frac{\text{Var}(f(w, w', x))}{\mathbb{E}(f(w, w', x))} < \infty$$

for all  $w' \in \mathring{W} \setminus W_0$ . If we work in a local chart  $U$  in a resolution around a minimum  $w^*$  of the loss then  $\mathbb{E}(f(w, w', x)) = u^{2k}$ , and we will see in the proof of Proposition E.37 that under the assumption  $f(w, w', x)$  also has Taylor expansion with leading term of order  $2k$ , so the ratio of the variance and expectation also converges to zero along as  $u \rightarrow 0$ .

We will assume below that  $q_w$  is a probability distribution for all  $w$ ; in particular that it is non-negative. If  $q_w = -\log p_w$  for a model  $p_w$ , as in the distribution learning example E.19, this is not generally true. In this case Proposition E.37 still holds in the realizable case by (Watanabe, 2009, Theorem 6.1) or under a more general relative finite variance condition as in (Watanabe, 2018, Theorem 8).

**Lemma E.39.** Let  $w^* \in W$  minimize the loss. If  $q_w$  is a probability distribution for all  $w$  and Assumption E.16 holds then

$$\mathbb{P}_{x \sim q_{w^*}}(g(x) \leq 0 | g(x)q_{w^*}(x) - h(x) = 0) = 0.$$

*Proof.* Since  $h(x) \geq 0$  and  $q_{w^*}(x) > 0$  almost surely, if  $g(x)q_{w^*}(x) - h(x) \geq 0$  then  $g(x) \geq 0$ . If  $g(x) = 0$  then  $g(x)q_{w^*}(x) - h(x) < 0$ , so by Assumption E.16 we conclude that  $g(x) > 0$  with probability one.  $\square$

*Proof of Proposition E.37.* Let  $w^* \in W$  be a point where  $G(w^*) = 0$ , and let  $X_{w^*} = \{x: g(x)q_{w^*}(x) - h(x) = 0\} \subseteq X$ . By Assumption E.16 we know that  $X \setminus X_{w^*}$  is a set of Lebesgue measure zero. We choose a log resolution  $\varpi$  and a chart  $U$  with coordinate  $u$  for which  $\varpi(0) = w^*$ . Then

$$\begin{aligned} u^{2k} &= G(\varpi(u)) \\ &= \int_X g(x)q_{\varpi(u)}(x) - h(x)dx \\ &= \int_{X_{w^*}} g(x)q_{\varpi(u)}(x) - h(x)dx \\ &= \int_{X_{w^*}} g(x) \left( \sum_{\alpha} b_{\alpha}(x)u^{\alpha} \right) - h(x)dx \\ &= \left( \int_{X_{w^*}} g(x)b_0(x) - h(x)dx \right) + \sum_{\alpha > 0} \left( \int_{X_{w^*}} g(x)b_{\alpha}(x) \right) u^{\alpha} \end{aligned}$$

where we use absolute convergence of the Taylor series to exchange the sum and the integral. By Lemma E.39  $g(x) > 0$  on  $X_{w^*}$  almost everywhere. Since  $b_{\alpha}(x)$  are the Taylor coefficients of a non-negative function, non-zero for some  $x \in X_{w^*}$ , the leading Taylor coefficient must be positive, and therefore  $b_{\alpha} = 0$  if  $0 < \alpha < 2k$ . The constant term  $b_0(x) = q_{w^*}(x)$ . Therefore

$$\begin{aligned} f(\varpi(u), w', x) &= \frac{q_{\varpi(u)}(x)}{q_{w'}(x)} g(x) - \frac{1}{q_{w'}(x)} h(x) \\ &= \frac{1}{q_{w'}(x)} \left( g(x)q_{w^*}(x) - h(x) + \sum_{\alpha \geq 2k} g(x)b_{\alpha}(x)u^{\alpha} \right) \\ &= f(w^*, w', x) + \frac{1}{q_{w'}(x)} \left( \sum_{\alpha \geq 2k} g(x)b_{\alpha}(x)u^{\alpha} \right). \end{aligned}$$

Finally, Assumption E.16 implies that  $f(w^*, w', x) = 0$ , and therefore the Taylor series of  $f(\varpi(u), w', x)$  in  $u$  is concentrated in degrees at least  $2k$ , and therefore in particular  $\omega_n = 0$  for all  $n$ .  $\square$

We may now study the asymptotic behavior of the generalized posterior distribution in terms of the geometry of the loss function  $G$ . We recall from Definition 2.1 the generalized tempered posterior distribution  $\Omega$ , the evidence  $Z_{n,\beta}(U)$  and free energy  $F_{n,\beta}(U)$ .

**Theorem E.40.** Suppose that  $q_w$  is a family of probability distributions and Assumption E.16 holds. Let  $U \subseteq W$  be an open subset, and let  $(\lambda, m) = (\text{rlct}_U(G), \text{rlcm}_U(G))$  denote the real log canonical threshold and multiplicity of the loss function  $G$  on the subset  $U$ . Then

$$Z_{n,\beta}(U) = C(\beta, \varphi|_U) n^{-\lambda} (\log n)^{m-1} + o_P(n^{-\lambda} (\log n)^{m-1})$$

where  $C(\beta, \varphi|_U)$  is constant in  $n$ .

**Remark E.41.** One can give an explicit integral formula for  $C(\beta, \varphi)$  as a sum over local charts in a log resolution, see (Watanabe, 2018, Section 6.3) or (Watanabe, 2009, Section 6.2) for such an expression.

*Proof.* Given Proposition E.37 and Theorem E.36 this follows from Watanabe's argument from (Watanabe, 2009, Theorem 6.7).  $\square$

**Corollary E.42.** We have convergence in distribution

$$F_{n,\beta}(U) - \lambda \log n + (m-1) \log \log n \rightarrow F_{\beta}(U)$$

for a random variable  $F_{\beta}(U)$  depending on  $\beta$  and the prior  $\varphi$ .

### E.2.5 Expected Total Loss and the Widely Applicable Bayesian Information Criterion

We will now conclude our technical arguments by establishing part (3) of Theorem E.24, the analogue of the *widely applicable Bayesian information criterion* Watanabe (2013), explaining how the generalized posterior selects between different critical regions of  $W_0$  as the number  $n$  of datapoints increases.

We will establish the following.

**Theorem E.43.** Suppose that  $q_w$  is a family of probability distributions and Assumption E.16 holds. Let  $\beta: \mathbb{N} \rightarrow \mathbb{R}_{>0}$  be a positive function on the natural numbers such that  $\beta(n)$  converges as  $n \rightarrow \infty$ . Let  $w^*$  be a local minimum of the loss and let  $U$  be an open neighborhood of  $w^*$  in  $W$ . Then

$$\frac{n\beta}{Z_{n,\beta}(U)} \int_U (G_n(w) - G_n(w^*)) \exp(-n\beta G_n(w)) \varphi(w) dw \rightarrow \lambda$$

in probability as  $n \rightarrow \infty$ , where  $\lambda = \text{rlct}_U(G)$  is the real log canonical threshold of the loss function.

*Proof.* We will follow the argument in (Watanabe, 2013, Theorem 4) closely. It suffices to work locally in  $W$ ; choose a local log resolution  $\varpi: \mathcal{M} \rightarrow W$  and a local chart  $V$  with local coordinate  $u$  centered around a preimage of  $w^*$ . Choose the chart so that  $G_0 = G(\varpi(0))$  is the minimum value of  $G \circ \varpi$  on  $V$ . Let  $\tilde{f}(w, w', x) = f(w, w', x) - G_0$  and  $\tilde{G}_n = G_n = G_0$ . Then

$$\frac{n\beta}{Z_{n,\beta}(U)} \int_{\varpi(V)} (G_n(w) - G_n(w^*)) \exp(-n\beta G_n(w)) \varphi(w) dw = \frac{n\beta}{\tilde{Z}_{n,\beta}(U)} \int_{\varpi(V)} \tilde{G}_n(w) \exp(-n\beta \tilde{G}_n(w)) \varphi(w) dw$$

where  $\tilde{Z}_{n,\beta}$  denotes the evidence with respect to the normalized posterior  $\exp(-n\beta \tilde{G}_n(w)) \varphi(w) dw$ .

We will study the numerator and denominator of our WBIC expression separately. Since we have established Proposition E.37 and Theorem E.36 Watanabe's calculations of these two expressions continue to apply in our setting; that is, by the argument in the proof of (Watanabe, 2013, Theorem 4) we have asymptotic behavior

$$\int_{\varpi(V)} \tilde{G}_n(w) \exp(-n\beta \tilde{G}_n(w)) \varphi(w) dw = C(\varphi) \log(n\beta)^{m-1} (n\beta)^{-\lambda-1} \Gamma(\lambda+1) + o_P(\log(n\beta)^{m-1} (n\beta)^{-\lambda-1})$$

$$\text{and } \tilde{Z}_{n,\beta} = \int_{\varpi(V)} \exp(-n\beta \tilde{G}_n(w)) \varphi(w) dw = C(\varphi) \log(n\beta)^{m-1} (n\beta)^{-\lambda} \Gamma(\lambda) + o_P(\log(n\beta)^{m-1} (n\beta)^{-\lambda})$$

as  $n \rightarrow \infty$ . So

$$\begin{aligned} \frac{n\beta}{\tilde{Z}_{n,\beta}(U)} \int_{\varpi(V)} \tilde{G}_n(w) \exp(-n\beta \tilde{G}_n(w)) \varphi(w) dw &\rightarrow n\beta \frac{C(\varphi) \log(n\beta)^{m-1} (n\beta)^{-\lambda-1} \Gamma(\lambda+1)}{C(\varphi) \log(n\beta)^{m-1} (n\beta)^{-\lambda} \Gamma(\lambda)} \\ &= \lambda \end{aligned}$$

as  $n \rightarrow \infty$  as required.  $\square$

**Remark E.44.** In Watanabe (2013) Watanabe uses the specific form  $\beta = \beta_0 / \log(n)$  for comparison with the free energy of the Bayesian posterior. That is for  $\mathcal{F}_{n,\beta_0}(U)$  as defined in Corollary E.42 we have

$$\mathcal{F}_{n,\beta_0}(U) - \mathbb{E}_n^\beta(nG_n(w)|_U) = o_P(\log n)$$

by Theorem E.43. The term *widely applicable Bayesian information criterion* (WBIC) is used for this expression since it generalizes the classical Bayesian information criterion Schwarz (1978), which this result recovers in the regular case.

## F Theory of LLC Estimation in Reinforcement Learning

**Definition F.1.** Let  $w^* \in W$  be a local minimum of the loss function  $G$ . The *local learning coefficient* of the optimization problem associated to  $G$  is the real log canonical threshold of  $G$  at  $w^*$ . We will denote the local learning coefficient as  $\lambda(w^*)$ . Often we will just write  $\lambda$ , keeping the choice of minimum implicit.

**Remark F.2.** If  $U \subseteq W$  is an arbitrary subset we will sometimes write

$$\lambda(U) = \text{rlct}_U(G) = \inf_{w \in U} \text{rlct}_w(G).$$

If we choose a metric on  $W$  then we can view the LLC as arising by  $\lambda(w^*) = \lim_{\varepsilon \rightarrow 0} \lambda(B_\varepsilon(w^*))$ .

As we have seen from Theorem E.40 the local learning coefficient controls the local behaviour of the generalized Bayesian posterior distribution near the point  $w^*$  in the large  $n$  limit. In general when  $\dim W$  is very large we cannot expect to compute  $\lambda$  exactly, so in this section we will discuss statistical estimators that we will use to substitute for it. Our estimators are based on the local learning coefficient estimators developed in Lau et al. (2025).

## F.1 Asymptotically Unbiased Estimators

We will begin with those estimators for which we can establish good theoretical properties rigorously, and generalize from there to estimators over which we have less theoretical control but which are more practical to estimate in realistic examples. To start with we can use the WBIC – Theorem E.43 – to define asymptotically unbiased estimators for the local learning coefficient.

Given a sequence of samples  $x_i \sim q_{w_i}$  as in Definition E.18, choose  $\beta > 0$  and let  $\Omega_{n,\beta}$  be the normalized posterior distribution from Definition 2.1. Choose an open neighborhood  $U$  of  $w^*$  and a natural number  $T$  and let  $y_1, \dots, y_T$  be independent random variables from the restriction of the generalized tempered posterior to  $U$ :  $y_j \sim \Omega_{n,\beta}|_U$ .

**Definition F.3.** Fix an analytic prior distribution  $\varphi$  on  $W$ . Define a random variable, the *WBIC LLC estimator*, by

$$\hat{\lambda}_{\text{WBIC},\varphi}(U) = \frac{n\beta}{T} \sum_{j=1}^T (G(y_j) - G(w^*)).$$

**Proposition F.4.** The WBIC LLC estimator  $\hat{\lambda}_{\text{WBIC},\varphi}(U)$  converges in probability to  $\lambda(U)$ :

$$\lim_{n \rightarrow \infty} \lim_{T \rightarrow \infty} \hat{\lambda}_{\text{WBIC}}(U) \rightarrow_P \lambda(U)$$

for all choices  $\varphi$  of prior.

*Proof.* This follows from Theorem E.43. Indeed, by the weak law of large numbers

$$\begin{aligned} \hat{\lambda}_{\text{WBIC},\varphi}(U) &= \frac{n\beta}{T} \sum_{j=1}^T (G(y_j) - G(w^*)) \\ &\rightarrow n\beta \mathbb{E}_{n,\beta}(G(w)|_U - G(w^*)) \end{aligned}$$

where the expectation value is taken with respect to the generalized tempered posterior to  $U$ :  $y_j \sim \Omega_{n,\beta}|_U$ . Theorem E.43 then tells us that this expected value converges to  $\lambda(U)$  in probability as  $n \rightarrow \infty$ , as required.  $\square$

## F.2 The Annealed Posterior

Let's discuss a variant of the WBIC-based LLC estimator with the same limiting properties as we saw in Proposition F.4. We will replace the tempered posterior in our definition with the *annealed posterior* (see Seung et al. (1992) for a discussion of this concept from its origin in statistical mechanics).

**Definition F.5.** Fix a constant  $n\beta > 0$  and an analytic prior distribution  $\varphi$  on  $W$ . The *annealed posterior distribution*  $\Omega$  is the probability distribution on  $W$  defined by

$$\begin{aligned} \Omega_{n\beta}^{\text{ann}}(U) &= \frac{Z_{n\beta}^{\text{ann}}(U)}{Z_{n\beta}(W)} \\ \text{where } Z_{n\beta}^{\text{ann}}(U) &= \int_U \exp(-n\beta G(w)) \phi(w) dw \end{aligned}$$

for open sets  $U \subseteq W$ .

**Remark F.6.** We have used the term  $n\beta$  for the constant appearing in the definition suggestively and for comparison with the tempered posterior, but we observe that the annealed posterior does not depend on the values of  $n, \beta$  separately.

**Proposition F.7.** Fix a log resolution and a chart  $U$  with local coordinate  $u$  as in Theorem E.36. Then

$$e^{-\frac{\beta \|\xi_n\|_\infty^2}{2}} Z_{\frac{n}{2}, \beta}(\varpi(U)) \leq Z_{n\beta}^{\text{ann}}(\varpi(U)) \leq e^{\frac{\beta \|\xi_n\|_\infty^2}{2}} Z_{\frac{3n}{2}, \beta}(\varpi(U)).$$

*Proof.* This follows from Proposition E.37 and the Cauchy–Schwartz inequality.  $\square$

We may therefore define a parallel version of the WBIC LLC estimator using the annealed posterior instead of the usual tempered posterior with good control of its behaviour in the large  $n\beta$  limit.

**Definition F.8.** Fix an analytic prior distribution  $\varphi$  on  $W$  and let  $y_1, \dots, y_T$  be independent random variables from the restriction of the annealed posterior to  $U$ :  $y_j \sim \Omega_{n\beta}^{\text{ann}}|_U$ . Define the *annealed WBIC LLC estimator* by

$$\hat{\lambda}_{\text{WBIC}, \varphi}^{\text{ann}}(U) = \frac{n\beta}{T} \sum_{j=1}^T (G(y_j) - G(w^*)).$$

The following is then a consequence of Proposition F.4 and the bound in Proposition F.7.

**Corollary F.9.** The annealed WBIC LLC estimator  $\hat{\lambda}_{\text{WBIC}, \varphi}^{\text{ann}}(U)$  converges in probability to  $\lambda(U)$ :

$$\lim_{n \rightarrow \infty} \lim_{T \rightarrow \infty} \hat{\lambda}_{\text{WBIC}}^{\text{ann}}(U) \rightarrow_P \lambda(U)$$

for all choices  $\varphi$  of prior.

### F.3 Soft Localization to an Open Set

For our next simplification we'll deal with the difficulty of directly imposing the restriction of samples to an open neighborhood  $U$  of  $w^*$ . We'll deal this in practice by judicious choice of the prior  $\varphi$  on  $W$ , following (Lau et al., 2025, Section 4.2). Choose an embedding  $\iota: W \hookrightarrow \mathbb{R}^D$  for some natural number  $D$  and define  $\varphi_{\sigma^2}$  by restricting a  $D$ -dimensional Gaussian centered at  $\iota(w^*)$  with variance  $\sigma^2$  to  $W$ .

**Remark F.10.** In Lau et al. (2025) the prior is instead parameterized by a fundamental scale parameter: the reciprocal of the variance  $\gamma = \sigma^{-2}$ . We'll avoid this notation to avoid conflict with the discount factor occurring in the reward function of a Markov decision problem.

**Definition F.11.** Fix  $n, T \geq 1$ , a local minimum  $w^*$  of the loss and a variance  $\sigma^2 > 0$ . Denote by  $\hat{\lambda}_{\sigma^2}(w^*)$  the random variable  $\hat{\lambda}_{\text{WBIC}, \varphi_{\sigma^2}}^{\text{ann}}(X)$ .

Since  $\varphi_{\sigma^2}$  is still supported everywhere on  $W$  Corollary F.9 still applies and the large  $n\beta$  limiting behaviour of the estimator is independent of  $\sigma^2$  in probability. The rate of convergence, however, depends on the value of  $\sigma^2$ : for any open neighborhood  $U$  of  $w^*$ , any  $n\beta, T$  and any  $\varepsilon > 0$  we can choose  $\sigma^2$  small enough that the samples  $y_1, \dots, y_T$  are all contained in  $U$  with probability  $> 1 - \varepsilon$ .

### F.4 Estimators from Stochastic Gradient Langevin Dynamics

We will now discuss the LLC estimators that are practically computable, corresponding to the estimator defined in (Lau et al., 2025, Section 4.4). These estimators are defined using *stochastic gradient Langevin dynamics* (SGLD) Welling and Teh (2011) as a substitute for sampling from the generalized posterior associated to the Gaussian prior  $\varphi_{\sigma^2}$ .

Given an initial point  $w^* \in W$  we will define a sequence  $w_1, \dots, w_T$  of points in  $W$  as follows. Fix a step size  $\varepsilon > 0$ . Then we let  $w_1 = w^*$ , and for  $j > 1$  define

$$w_j = w_{j-1} + \frac{\varepsilon}{2} \left( \frac{n\beta}{m} \sum_{i=1}^m \nabla_w f(w, w_j, x_{j,i})|_{w=w_j} + \frac{1}{\sigma^2} (w^* - w_j) \right) \quad (19)$$

where  $m$  is a natural number (the *batch size*) and  $x_{j,1}, \dots, x_{j,m}$  are a sequence of independent samples from  $q_{w_j}$ .

Let us comment briefly on the motivation behind this idea. Roberts and Tweedie (1996) study the *Langevin diffusion* stochastic differential equation associated to a probability distribution  $\pi$  on  $\mathbb{R}^D$

$$dL_t = \frac{1}{2} \nabla \log \pi(L_t) dt + dW_t$$

where  $W_t$  is a standard Brownian motion on  $\mathbb{R}^D$ . They argue that under a continuity condition for  $\pi$  together with a mild growth condition along rays the Langevin diffusion equation admits  $\pi$  as its unique invariant distribution (Theorem 2.1 in *loc. cit.*). Therefore, in our applications, the generalized (annealed) posterior distribution from which we need to be sampled can be obtained by flowing with respect to the Langevin diffusion.

In order to reify this idea the idea is to use a suitable discrete approximation to the continuous Langevin diffusion: this is the role played by Welling and Teh's stochastic gradient Langevin descent.

**Remark F.12.** We mention here some open problems related to the behaviour of SGLD in singular learning theory; we refer the reader to Hitchcock and Hoogland (2025) for a more detailed discussion.

1. SGLD with constant step size is known, even under strong convexity assumptions on the objective function, to have limiting behaviour that differs from that of Langevin flow (as shown, for instance, in Brosse et al. (2018)). Therefore the SGLD based estimator is likely to be asymptotically biased with bias depending on the step size  $\varepsilon$ . Can this bias be quantified?
2. If one uses decaying step size then there are results implying almost sure convergence to the posterior distribution as the chain length  $T \rightarrow \infty$  Teh et al. (2016). These results, however, make assumptions that do not typically hold for the neural network models we are most interested in (see (Hitchcock and Hoogland, 2025, Appendix B) for a detailed discussion). What can one say upon relaxing these assumptions?

**Remark F.13.** Notice that in our implementation of SGLD we sample trajectories at each step in the chain *on-policy*. In other words in equation 19 we use the derivative  $\nabla_w f(w, w_j, x_{j,i})|_{w=w_j}$  at step  $j$  and not  $\nabla_w f(w, w^*, x_{j,i})|_{w=w_j}$ . Recall that these two random variables have the same expected value but generally different higher moments. Either choice would provide an estimator for the gradient flow term in the Langevin diffusion for the annealed posterior; we choose to use on-policy sampling since it typically has lower variance.

If we use a subsequence  $w_B, \dots, w_T$  for some initial point  $B > 0$  (the *burn-in* parameter) as a substitute for sampling from the posterior distribution  $\exp(-n\beta G_n(w))\varphi_{\sigma^*}(w)dw$  on  $W$  then we obtain the estimator that we compute in practice by analogy with the one defined in Definition F.11. For convenience we summarize the hyperparameters that this estimator depends on a table below.

| Notation                          | Description              |
|-----------------------------------|--------------------------|
| $w^* \in W$                       | Initial point in $W$     |
| $\beta \in \mathbb{R}_{>0}$       | Inverse temperature      |
| $n \in \mathbb{N}$                | Number of training steps |
| $\sigma^2 \in \mathbb{R}_{>0}$    | Noise variance           |
| $T \in \mathbb{N}$                | SGLD chain length        |
| $\varepsilon \in \mathbb{R}_{>0}$ | SGLD step size           |
| $m \in \mathbb{N}$                | SGLD batch size          |
| $B \in \mathbb{N}$                | Number of burn-in steps  |

Table 2: A list of the hyperparameters on which the random variable  $\hat{\lambda}_{\text{SGLD}}(w^*)$  depends. Note that the estimator does not depend on  $n$  and  $\beta$  independently, only on their product  $n\beta$ .

**Definition F.14.** The *SGLD based LLC estimator*  $\hat{\lambda}_{\text{SGLD}}(w^*)$  is defined by

$$\hat{\lambda}_{\text{SGLD}}(w^*) = \frac{n\beta}{T} \sum_{j=B}^T (G_n(w_j) - G_n(w^*)).$$

## G Further LLC Estimate Data

In this appendix we present our LLC estimates during training for models trained while varying the hyperparameters  $\alpha$  and  $\gamma$  and while keeping these hyperparameters fixed and varying the random seed. We present four ensembles of figures.

- Figure 9 shows LLC estimates for independently sampled models with  $\gamma = 0.975$  and  $\alpha = 0.68$ , with LLC estimation performed on distribution, i.e. with the same hyperparameters.
- Figure 10 shows LLC estimates for models where estimation was performed with  $\gamma = 0.98$  and  $\alpha = 0.5$ .
- Figure 11 shows LLC estimates for models where estimation was performed with  $\gamma = 0.98$  and  $\alpha = 0$ .
- Figure 12 compares the LLC estimates with  $\gamma = 0.98$  and  $\alpha = 0.5$  to the weight norms of the model. We see that the weight norms are distinct from the LLC estimates. In particular they always increase monotonically during training and do not reflect the phase transitions to as significant an extent as the LLC estimates.

## H Nonlinear relationship between LLC estimates and regret

Looking at Figure 9 one might be concerned that the LLC is approximately a linear function of the regret. To see that this is not the case it is sufficient to show that the average (regret, LLC estimate) pairs in the three phases are not collinear (although we do additionally observe non-linear development *within* the phases). To test this we define the random variable

$$d = \frac{\hat{\lambda}_{2b} - \hat{\lambda}_1}{G_{2b} - G_1} - \frac{\hat{\lambda}_3 - \hat{\lambda}_{2b}}{G_3 - G_{2b}}$$

where  $\hat{\lambda}_i$  and  $G_i$  are the average LLC estimates and average regrets among checkpoints in phase  $i$  respectively. Under the hypothesis that  $G_i$  and  $\hat{\lambda}_i$  are linearly related the random variable  $d$  would have expected value zero for all  $\alpha$  and  $\gamma$  values. We may test this using the mean of  $d$  across a set of independent samples with fixed  $\alpha$  and  $\gamma$ . We have 21 runs with  $\alpha = 0.68$  and  $\gamma = 0.975$ , and show the distribution of  $d$  for llcs computed on-distribution in Figure 13. Since these samples are iid we may perform a one sample t-test and reject the hypothesis that  $\mathbb{E}(d) = 0$  with significance  $p = 0.00005$ .

## I Sensitivity of automatic phase detection

In Section 3.4.1 we described a natural function by which one can automatically detect when the training process has entered a phase by measuring the distance in policy space between the current policy  $\pi$ , and the closest example policy  $\pi'$  contained in some subspace  $P$ . If the distance is below some fraction  $\delta$  of its maximum value then we say that  $\pi$  has approximately entered the phase associated with the subspace of policies  $P$ . In other words we detect the phase associated to  $P$  when

$$\min_{\pi' \in P} \|\pi - \pi'\| < \delta d_P$$

where  $d_P = \max_{\pi} \max_{\pi' \in P} \|\pi - \pi'\|$  is the maximum distance from the subspace  $P$ .

From Figure 14 we can see that for  $0.10 \leq \delta \leq 0.16$  the number of checkpoints between phase transitions is roughly constant (recall that spacing between checkpoints is logarithmic). In particular our LLC estimates within each phase are not significantly sensitive to the value of the threshold  $\delta$  within this range.

When  $\delta$  exceeds 0.16, we spuriously detect phase 2b early – our threshold has exceeded the distance between the two phases. Since we only include training runs where all three phases are present, for values of  $\delta$  sufficiently small the sample size begins to decrease as fewer samples exceed the threshold for detecting the middle phase at some point during training; this is why the plots are not monotonic. Below  $\delta = 0.05$ , no phases are detected in any of the runs, and the average is undefined.

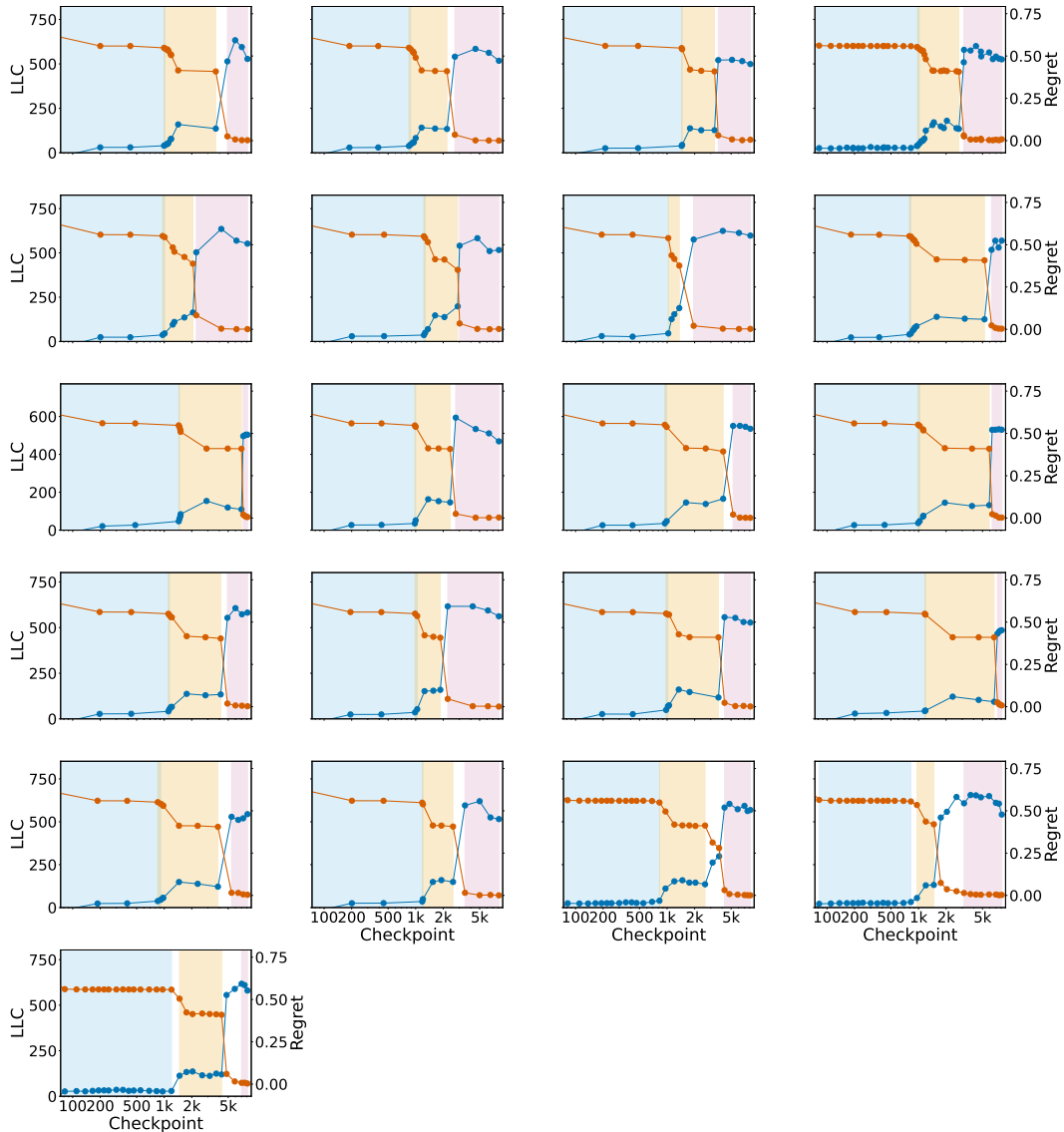


Figure 9: On-distribution LLC (blue line) estimated with  $\gamma = 0.975$  and  $\alpha = 0.68$  for runs with different seeds. The brown curve shows the regret, and the blue, beige and pink regions indicate phase 1, 2b and 3 respectively.

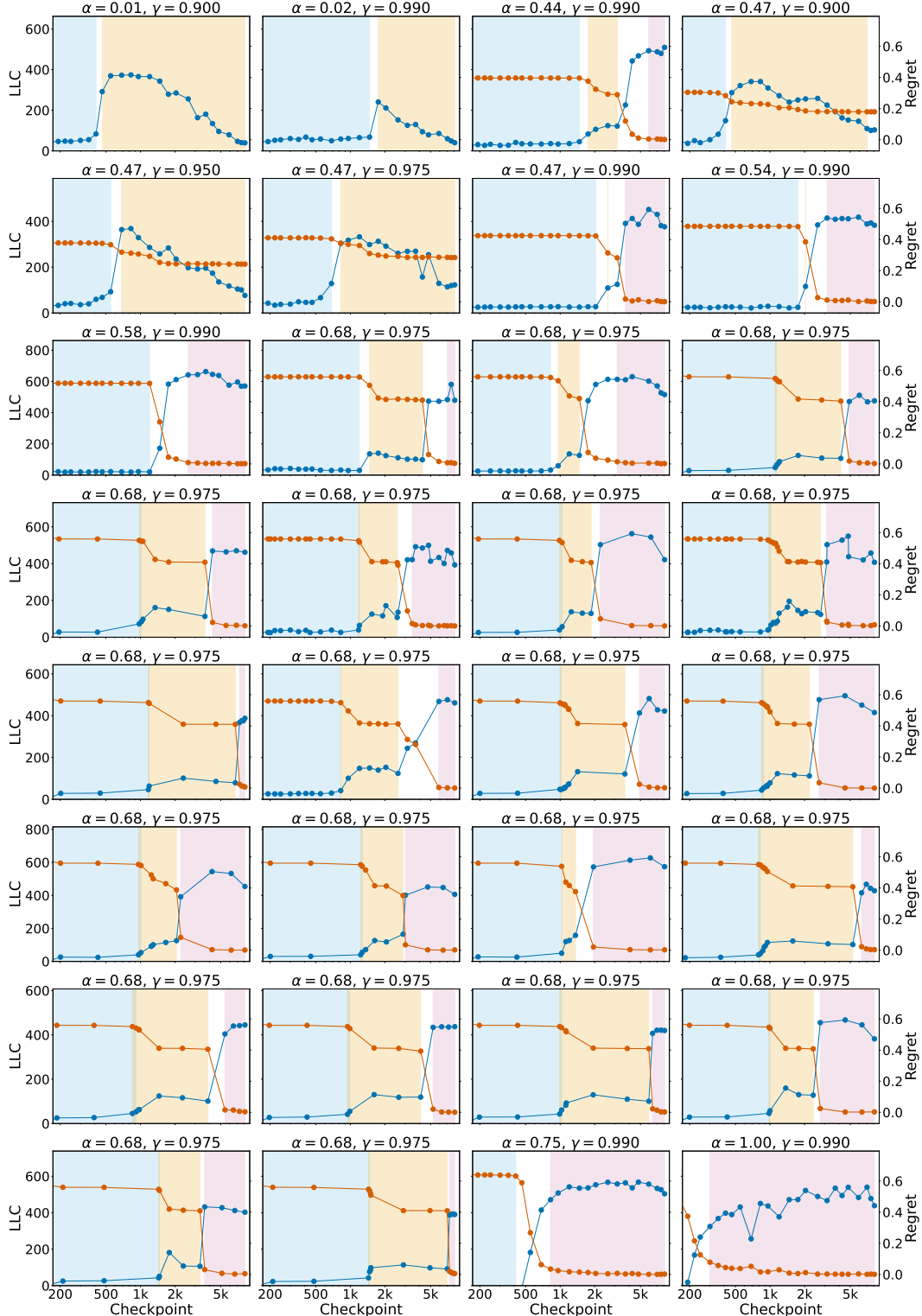


Figure 10: LLC (blue line) estimated with  $\gamma = 0.98$  and  $\alpha = 0.5$  for models trained with values of  $\alpha$  and  $\gamma$  indicated in the titles of the panels. The runs that share  $\alpha$  and  $\gamma$  differ only by the random seed with which they were trained. The brown curve shows the regret, and the blue, beige and pink regions indicate phase 1, 2b and 3 respectively.

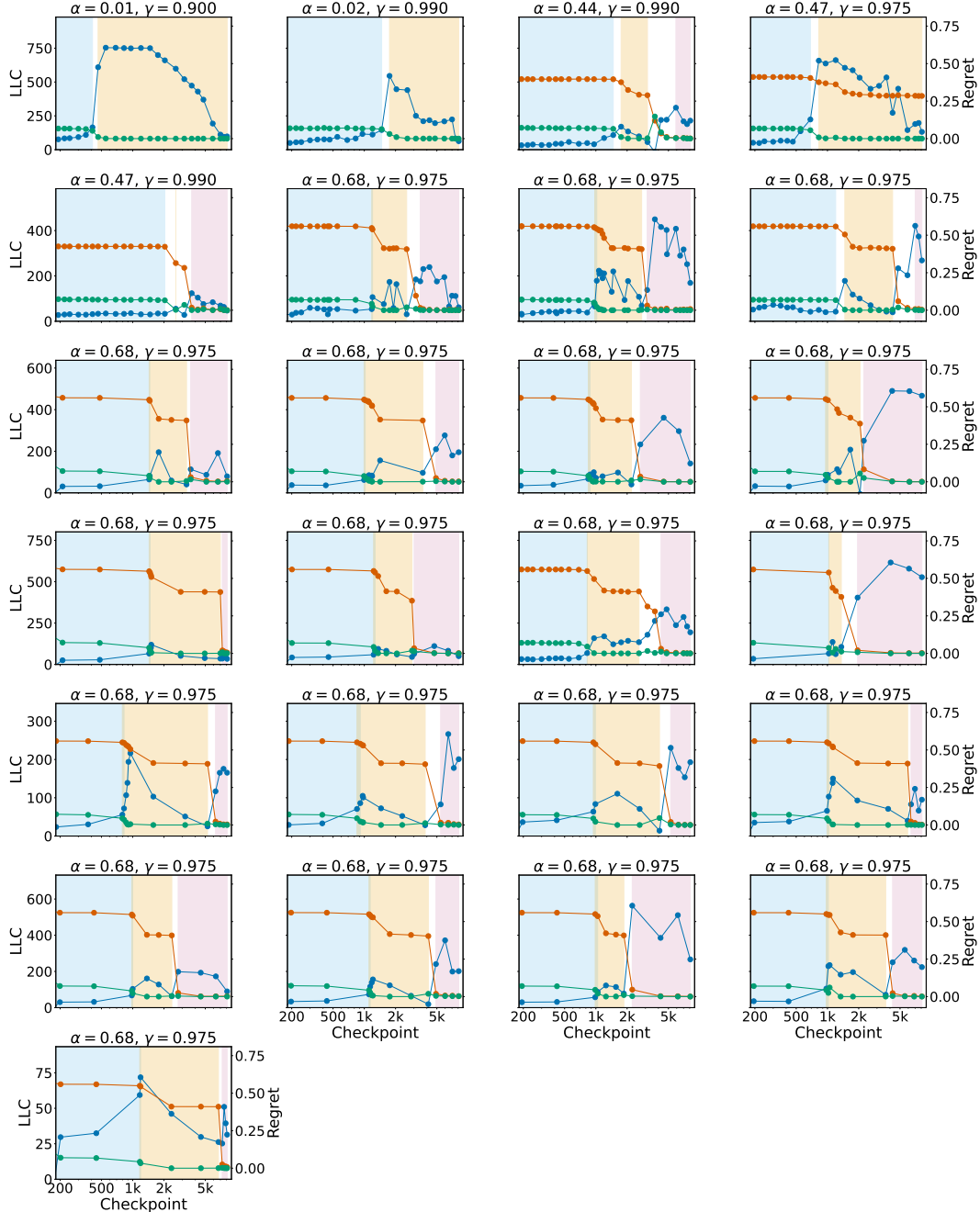


Figure 11: LLC (blue line) estimated with  $\gamma = 0.98$  and  $\alpha = 0$  for models trained with values of  $\alpha$  and  $\gamma$  indicated in the titles of the panels. The runs that share  $\alpha$  and  $\gamma$  differ only by the random seed with which they were trained. The brown curve shows the regret, and the blue, beige and pink regions indicate phase 1, 2b and 3 respectively.

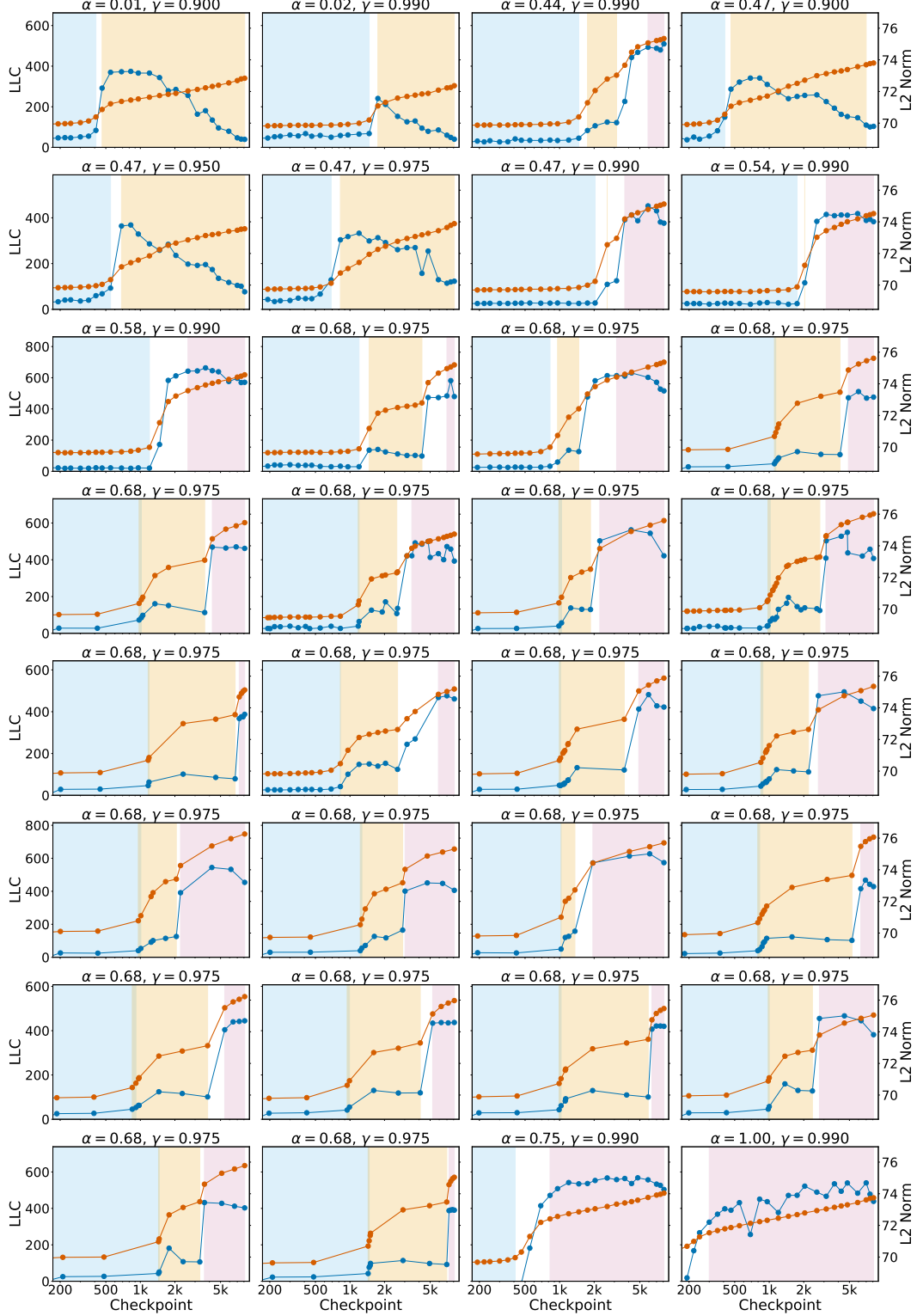


Figure 12: LLC estimates (blue curves) with  $\gamma = 0.98$  and  $\alpha = 0.5$  for models trained with values of  $\alpha$  and  $\gamma$  indicated in the titles of the panels. The runs that share  $\alpha$  and  $\gamma$  differ only by the random seed with which they were trained. The shaded areas indicate the phase the model is in, with blue, beige and pink indicating phases 1, 2b and 3 respectively. These plots also show the weight norms (orange curves), which monotonically increase throughout training.

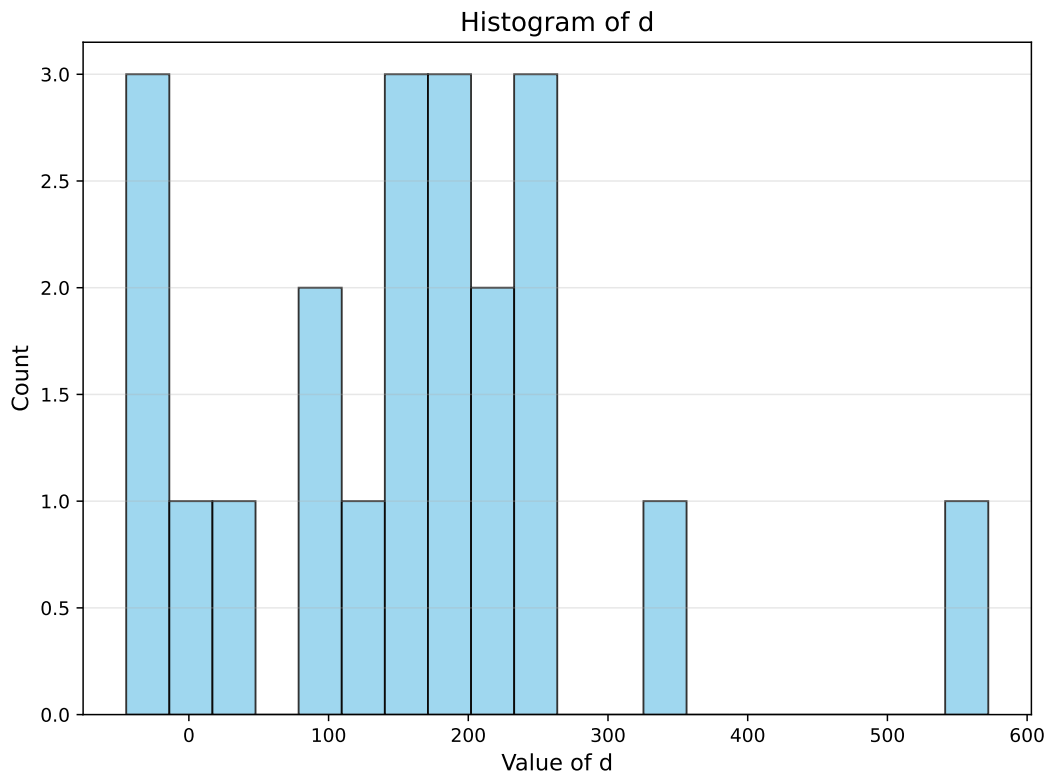


Figure 13: Distribution of the random variable  $d$  representing the difference in the rate of change of the LLC estimate with respect to the regret between phases 1 and 2b, and between phases 2b and 3, measured across 21 different iid runs for which  $\gamma = 0.975$  and  $\alpha = 0.68$ .

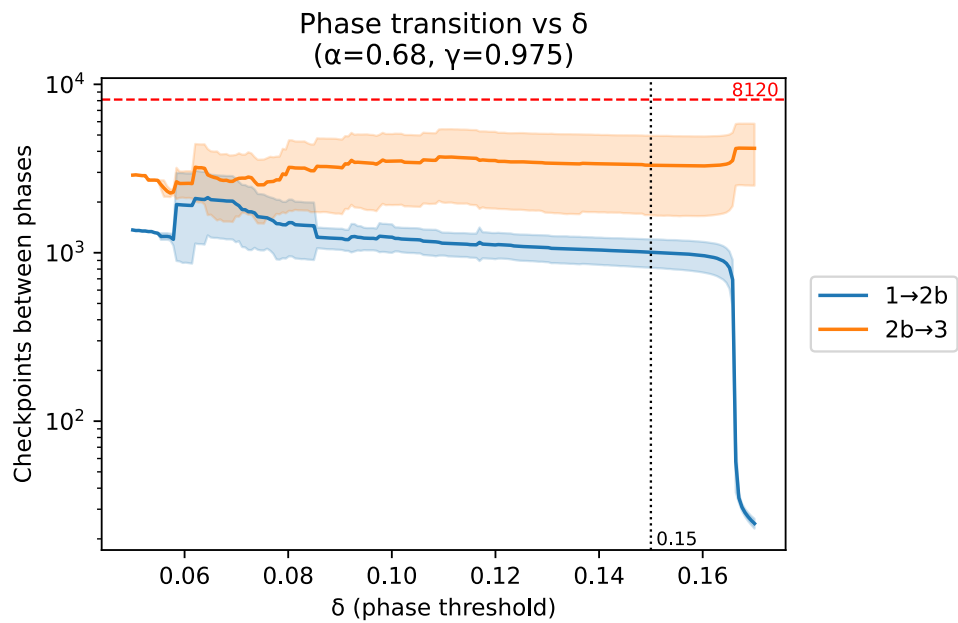


Figure 14: A plot showing the average number of checkpoints between Phase 1 and Phase 2b (blue), and the average number of checkpoints between Phase 2b to Phase 3 (orange). Models were trained with hyperparameters  $\alpha = 0.68, \gamma = 0.975$ . Training runs are only included if the policy was detected to be in all of phase 1, phase 2b and phase 3 at some point during training.